Use of Guard/Girder/Restraining Rail

DETAILS

38 pages | | PAPERBACK
ISBN 978-0-309-43646-5 | DOI 10.17226/23186

AUTHORS

April 2007

TRANSIT COOPERATIVE RESEARCH PROGRAM
Sponsored by the Federal Transit Administration

Subject Areas: VI Public Transit, VII Rail

Responsible Senior Program Officer: Christopher W. Jenks

Research Results Digest 82

USE OF GUARD/GIRDER/RESTRAINING RAILS

This digest summarizes the results of TCRP Project D-7/Task 12, "Restraining/Guard Rail." The digest was prepared by the Transportation Technology Center, Inc. (TTCI), Pueblo, Colorado. Xinggao Shu and Nicholas Wilson served as principal authors.

CONTENTS

Summary, 1

1 Introduction, 2

2 Guard/Girder/Restraining Rail Practices Survey, 3
- 2.1 Guard/Girder/Restraining Rail Structure and Layout, 4
- 2.2 Guard/Restraining Rail Installation Curve Radius, 5
- 2.3 Flangeway Width, 6
- 2.4 Guard/Restraining Rail Height, 7
- 2.5 Rail Lubrication, 8
- 2.6 Summary of the Survey, 8

3 Three-Dimensional W/R Contact Geometry, 8
- 3.1 Wheel with a 75-Degree Flange Angle, 8
- 3.2 Wheel with a 63-Degree Flange Angle, 10

4 Guard/Girder/Restraining Rail Parameter Optimization, 10
- 4.1 Optimization Objective Functions: W/R Interaction Forces and Wear, 11
- 4.2 Single Wheelset Simulation Model, 11
- 4.3 Guard Rail, 12
- 4.4 Girder Rail, 21
- 4.5 Restraining Rail, 22

5 Validation through Transit Vehicle Simulations, 29
- 5.1 Vehicle Negotiating a Curve with a Guard Rail, 29
- 5.2 Vehicle Negotiating a Curve with a Girder Rail, 30
- 5.3 Vehicle Negotiating a Curve with a Restraining Rail, 30

6 Vehicle Safety and Wear Analysis for Guard/Girder/Restraining Rail Installation, 31
- 6.1 Safety Analysis, 31
- 6.2 Wear Analysis, 32

7 Conclusions, 33

8 Discussion and Future Work, 36
- 8.1 Discussion, 36
- 8.2 Future Work, 37

References, 37

Author Acknowledgments, 37

Preliminary guidelines are provided herein for the application of guard/girder/restraining rails by transit systems in order to improve vehicle curving performance, to reduce risk of flange climb derailment, and to control wheel/rail wear.

SUMMARY

The effects of three-dimensional wheel/guard/girder/restraining rail contact geometry and guard/girder/restraining rail installation parameters—including flangeway width and height, lubrication, track curvatures, track gage, and vehicle types on the wheel/rail (W/R) forces and wear—have been investigated through NUCARS® simulations. A number of important conclusions and guidelines for optimized guard/girder/restraining rail installation and design can be drawn from this work including the following:

- The optimal guard/girder/restraining rail installation, leading to a balance of lateral W/R forces as well as a balance of wear between the high rail and the guard/girder/restraining rail, can be achieved through the control of flangeway width and W/R friction coefficients.
- The optimal flangeway width depends on the wheel profile shape, including flange back profile, wheel back-to-back distance, track gage, guard/girder/restraining rail profile shapes, installation height, and wheelset angle of attack (AOA) or the track curvature.
- The optimal flangeway width makes the flange front W/R clearance between the wheel flange face and the high rail equal to the flange back clearance between the wheel flange back and the guard rail (see Figure 1 in Section 2.1).
- A wide flangeway leads to high lateral forces and wear on the high rail and increases high-rail flange climb derailment risk.
- A narrow flangeway leads to high lateral forces and wear on the guard/girder/restraining rail and increases low-rail flange back climb derailment risk.
- The flangeway should increase with the wheelset AOA and track curvature for AOA larger than 20 milliradians (mrad), which corresponds to curves with a radius of about 290 ft, if the three-dimensional flange back fattening effect is larger than the fattening effect on the maximum flange angle face (this situation applies to most W/R contact cases).

TRANSPORTATION RESEARCH BOARD
OF THE NATIONAL ACADEMIES

- Three-dimensional W/R contact effects are significant at AOA larger than 58 mrad (corresponding to curves with a radius of about 100 ft).
- The flangeway width should increase by approximately the same amount as the track gage to keep the flange front clearance equal to the flange back clearance. Increasing only the gage leads to excessive wear on the guard/girder/restraining rails.
- Increasing gage or decreasing flangeway width leads to a tendency of increasing lateral W/R forces and wear on guard/girder/restraining rails because increasing gage increases the W/R flange front clearance, and decreasing flangeway width decreases the flange back clearance, causing the guard/girder/restraining rail to contact the wheelset before the high rail contacts the flange face. Correspondingly, decreasing gage or increasing flangeway width leads to a tendency of increasing lateral W/R forces and wear on high rails.
- The flangeway width should increase with the increase of the guard/girder/restraining rail height to keep the flange front clearance equal to the flange back clearance.
- The total rolling resistance increases with the increase of the guard/girder/restraining rail height. However, the height effect for guard and girder rails on W/R wear and the rolling resistance is relatively small compared with that of the restraining rail.
- The restraining rail height has a significant effect on rolling resistance and W/R wear. The restraining rail should be installed low enough to mitigate excessive wear and decrease rolling resistances unless there are other safety concerns.
- Lubrication on the high-rail gage face and guard/girder/restraining rail significantly reduces the W/R wear and rolling resistances. To achieve similar wear rates between the high rail and the guard rail, the guideline for rail lubrication with guard rails is to produce low friction coefficients on the contact patches in the presence of high contact angles and relatively high friction coefficients on the contact patches in the presence of low contact angles.
- The wear for wheels with higher flange angles is more severe than those with lower flange angles under the same running and load conditions. The optimized guard/girder/restraining rail installations could provide solutions to excessive W/R wear.
- To ensure safety, the guideline for guard rail installations on curves is to install guard/girder/restraining rails wherever the wheel lateral-to-vertical (L/V) ratio and flange climb distance exceed the wheel L/V ratio and climb distance criteria as proposed in *TCRP Report 71: Track-Related Research—Volume 5: Flange Climb Derailment Criteria and Wheel/Rail Profile Management and Maintenance Guidelines for Transit Operations* (*1*). Either tests or simulations can provide the L/V ratio and climb distance.
- The consistency between the damage functions (*9*) and simulation results for vehicles in different transit systems shows that the rail damage functions and simulations can be used for W/R wear and economics analysis.

Research on the flangeway wear limits and maintenance tolerances are proposed for future work. This work should consider the effects of worn wheel and rail including guard/girder/restraining rail geometries.

1 INTRODUCTION

Guard/restraining rails are used in transit systems to reduce rail wear in sharp curves as well as to increase the track's resistance to flange climb derailment. Guard/restraining rails are also installed in track curves, where the high rail wears rapidly, as they are considered beneficial in reducing the frequency and cost of high-rail replacements.

TCRP Report 71: Track-Related Research—Volume 5: Flange Climb Derailment Criteria and Wheel/Rail Profile Management and Maintenance Guidelines for Transit Operations (*1*) shows that there are different practices for restraining rail installation and that design and maintenance standards vary among transit systems. This wide variety of practices, coupled with problems observed in the use of the guard/restraining rails, indicated that a detailed study of restraining rail designs and maintenance practices could be beneficial to all transit systems.

In 2005, Transportation Technology Center, Inc. (TTCI), in Pueblo, Colorado, was contracted by TCRP to develop preliminary guidelines for the application of guard/restraining rails by transit systems to improve vehicle curving performance, reduce risk of flange climb derailment, and control wear.

The tasks of this project were the following:

- Conducting a survey of the current uses of guard/restraining rail in transit systems, as well as examining and evaluating present guidelines;
- Investigating the effect of guard/restraining rail parameters on wheel/rail (W/R) forces and wear through NUCARS® simulation and analysis; and
- Providing preliminary guidelines for guard/restraining rail design and maintenance based on the survey results and NUCARS® simulation and analysis.

2 GUARD/GIRDER/RESTRAINING RAIL PRACTICES SURVEY

In the late nineteenth century, guard/restraining rails were commonly used in both railroad and transit systems because the locomotives in service at that time were likely to derail on sharp curves because of locomotives' long wheelbase. Through time, as the locomotive wheelbase was shortened, railroads gradually eliminated rails on curves; however, they were still used on switches and frogs. Transit systems, on the other hand, continued the use of guard/restraining rails on switches, frogs, and curves. The following factors lead to guard/restraining rails being more commonly used on curves in transit systems than in railroad operations:

- Sharp curves—transit systems have sharper curves than most railroads;
- High traffic densities—transit systems have frequent trains and very limited time periods for track maintenance, making replacement of worn running rails difficult;
- Narrow wheel treads—many transit systems have wheel treads that are narrower than regular railroad wheels, making them much more sensitive to the gage-widening effects of gage face wear in curves; and
- Independent rotating wheel (IRW)—the use of IRW in some transit cars increases the risk of flange climb derailment.

Guard/restraining rail design and maintenance standards in transit systems came from railroad industry practices. Guard/restraining rails on railroads, however, were mainly used on switches and frogs where no rail cant existed. Guard/restraining rail design and maintenance standards for curves had to differ from those for switches and frogs because of their different running surroundings and functions. Also, because of the variety of vehicle designs and track gages, standards varied among transit systems. General guard/restraining rail installation guidelines are needed for transit systems to develop their own industry-specific standards.

The American Public Transportation Association (APTA) and antecedent organizations have been effective in sponsoring, producing, or assisting in the collection of data for publications aimed partly at improving track systems and standardizing them when that is economically efficient.

In September 1979, the Track Construction and Maintenance Subcommittee submitted to APTA a recommendation for a study of restraining rails accompanied by an outline of the scope of work required to develop guidelines. ENSCO, Inc., was contracted by the Urban Mass Transportation Administration (UMTA) for this study under the UMTA Urban Rail Construction Technology Program.

A survey of nine U.S. transit properties and the Toronto Transit Commission was conducted during the study (*2, 3*). The report evaluated the benefits of alternative practices, presented concepts for advanced designs, discussed simplified analysis of the costs and benefits of restraining rail installations, recommended the design and fabrication of modifications and concepts, and recommended tests to obtain additional information for improvements in track adjustment and practices in order to reduce rail wear.

Based on the practices survey and analysis, some guidelines for the use of restraining rail were compiled under that project and were presented in a report entitled *U.S. Transit Track Restraining Rail—Volume II: Guidelines* (*3*).

In May 1982, under the same program, a transit car test on a tight loop curve with a 150-ft radius was conducted at the Transportation Test Center (TTC) in Pueblo, Colorado, to investigate the effects of lubrication on restraining rails and high rails of curves (*4*).

In 2000, *TCRP Report 57: Track Design Handbook for Light Rail Transit* was published (*4*). This handbook provides guidelines and descriptions for the design of various types of light rail transit track. The track structure types covered include ballasted, direct-fixation (ballastless), and embedded track. The components of the various track types are discussed in detail. The guidelines consider the characteristics and interfaces of vehicle wheels and rail, track

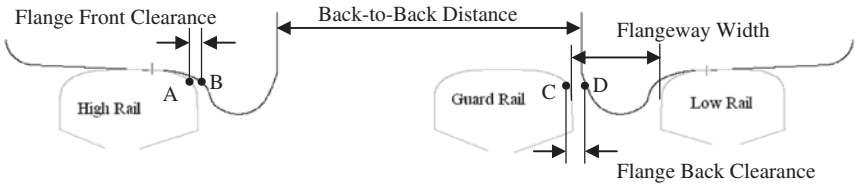

Figure 1 W/R contact with guard rail.

and wheel gages, rail sections, alignments, speeds, and track moduli.

The Transportation Technology Center, Inc. (TTCI), has studied vehicle curving with restraining rails in the past (*5, 6*) and undertook TCRP Project D-7/Task 12, "Restraining/Guard Rail Study." As one of the tasks of this project, a questionnaire was sent to several transit systems for the current restraining rail practice survey.

In the following sections, information compiled from a literature review, a previous TCRP project survey, and the questionnaire survey for this project is presented. Several critical design and maintenance standards, such as the restraining rail installation curve radius, flangeway width, and restraining rail height, are examined against the corresponding guidelines.

2.1 Guard/Girder/Restraining Rail Structure and Layout

Four types of guard/girder/restraining rails, commonly used in transit systems, are shown in Figures 1 through 5 with typical structures and layouts. Standard tee rails are used for the guard/restraining rail structures, as Figures 1 and 2 show. These guard/restraining rails are installed in a vertical or horizontal position according to design practices that have been standardized by individual transit properties (based on local experience). The rails are readily available for the restraining rail, including worn rails that have been removed from track.

Figure 1 shows the contact points on the wheels/rails. Point "A" is the contact point on the high-rail gage corner; Point "B" is the contact point on the high-rail wheel flange root; Point "C" is the contact point on the guard rail; Point "D" is the contact point on the low-rail wheel flange back. The wheel/rail/guard rail geometry parameters are defined in Figures 1 and 2, and these parameters will be referenced in the following sections.

The most common type of guard rail is a vertically mounted tee rail with about a 70- to 80-degree contact angle on the wheel flange back, as Figure 1 shows. The horizontal mounted tee rail, shown in Figure 2, makes contact with the wheel on the wheel back with a 90-degree contact angle. NUCARS® models these two structures as two different W/R contact models. In this digest, rails with a 70- to 80-degree contact angle on the wheel flange back, as Figure 1 shows, are referred to as guard rails; rails with a 90-degree contact angle on the wheel back, as

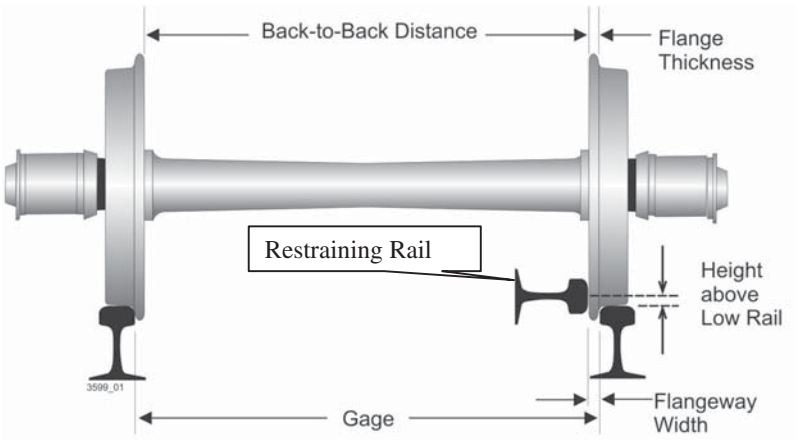

Figure 2 Wheel and horizontal restraining rail geometry.

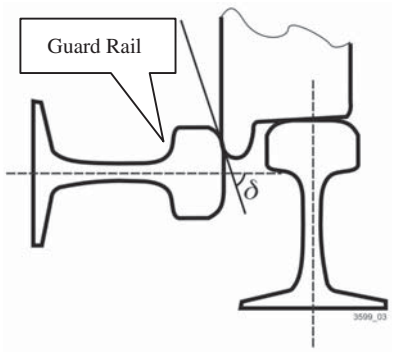

Figure 3 Wheel and horizontal guard/restraining rail installed at low position.

Figure 2 shows, are referred to as restraining rails. According to this definition, the horizontal mounted rail with low height in Figure 3 is modeled as a guard rail because its contact angle, δ, on the wheel flange back is less than 90 degrees.

The girder rail shown in Figure 4 and the strap guard rail shown in Figure 5 are used by some light rail transit systems. The strap guard rail is an alternative to girder rail for the convenience of fabrication and installation.

The girder rail is used both on high and low rail on the concrete pavement way to keep the flangeway on both rails. Some transit systems place a guard or restraining rail adjacent to the high rail and the low rail on extremely sharp curves. In a double restraining rail installation, the restraining rail alongside the inner rail shifts the leading axle of the truck toward the center of the curve. The outer restraining rail then guides the trailing axle away from the center, helping to ensure that the truck is reasonably square to the track, that both axles are in a nearly radial orientation, and that the truck frame is rectilinear rather than warp. In this digest, only the guard/girder/restraining rail on the low rail is modeled. However, the same methodologies can be applied to the guard/girder/restraining rail on the high rail.

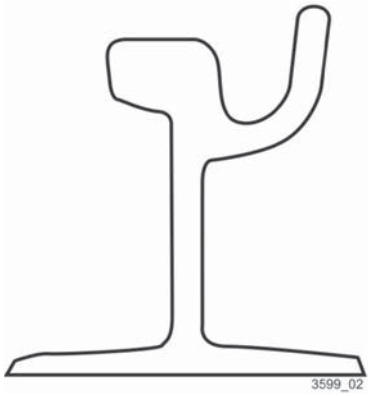

Figure 4 Girder rail.

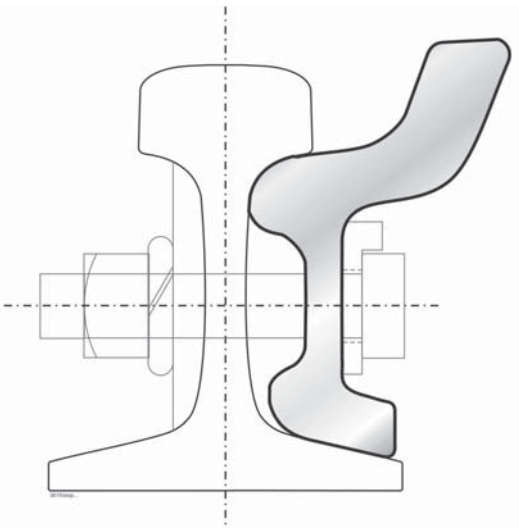

Figure 5 Strap guard rail.

The W/R contact geometry for these various guard/girder/restraining rail structures differs, especially when the three-dimensional contact features are considered. The horizontal restraining rail (see Figure 2) contacts the wheel on the wheel back, whereas the other three types of guard/girder/restraining rail usually contact the wheel on the back part of wheel flange tip, as Figure 1 shows. Detailed analyses of W/R contact geometry and its effect on W/R wear and wheelset steering performance are presented in the following sections.

2.2 Guard/Restraining Rail Installation Curve Radius

In *U.S. Transit Track Restraining Rail—Volume II: Guidelines* (*3*), installation of guard/restraining rails is recommended for the following:

- "all main line curves of a 500 ft radius or less; except where cars are operated at or below balanced speed and periodic inspections show that the wheels do not have tendencies to climb the high rail."
- "mainline curves above 500 ft radius where periodic inspections indicate the car wheels have tendencies to climb the high rail."

Table 1 Examples of guard/restraining rail installation practices

Transit System	Practice
MBTA (Light Rail Line)	Guard/restraining rail is installed on curves with a radius less than 1,000 ft.
Newark City Subway (Light Rail Line)	Guard/restraining rail is installed on curves with a radius less than 600 ft.
SEPTA (Heavy Rail Line)	Guard/restraining rail is installed on curves with a radius less than 750 ft.
WMATA (Heavy Rail Line)	Guard/restraining rail is installed on switches corresponding to less than 500 ft in radius and curves with a radius less than 775 ft.
CTA (Heavy Rail Line)	Guard/restraining rail is installed on curves with a radius less than 500 ft.

NOTE: MBTA = Massachusetts Bay Transportation Authority. SEPTA = Southeastern Pennsylvania Transportation Authority. WMATA = Washington Metropolitan Area Transit Authority. CTA = Chicago Transit Authority.

Table 1 shows the current practices used by several different transit systems.

It would be desirable to provide guidelines based on the track and vehicle information instead of periodic inspection because the decision to use or not use a guard/restraining rail has to be made during the design and test stage, and it is impractical for periodic inspection to occur at that time. However, it is advisable to install guard/restraining rails where periodic inspections show severe wear on the high rail on existing lines.

2.3 Flangeway Width

Two guidelines for flangeway width in *U.S. Transit Track Restraining Rail—Volume II: Guidelines* (*3*) are quoted below:

- "In an installation designed for the restraining rail to wear at the approximate rate of the lubricated high rail, the guard distance from the guard face of the restraining rail to the gage side of the high rail should equal the back-to-back distance between wheels plus one flange thickness."
- "In an installation designed for the restraining rail to prevent wear of the high rail, the guard distance should be 0.6 in. more than the back-to-back of wheels distance plus flange thickness."

Table 2 shows the current flangeway width design and maintenance standards from three transit systems. These three transit systems do not appear to use the two guidelines quoted above for flangeway width in their flangeway width specifications.

From a geometry point of view, the flangeway width depends on the W/R profiles, track gage, track curvature, and vehicle geometric characteristics such as the axle spacing in a truck. The appropriate gage and flangeway width to be used in curved track must be determined through an analytical process. One such geometric method is known as the "Filkins-

Table 2 Guard/restraining rail geometry dimensions on 700-ft radius curves from three transit systems

Geometry Parameters	Transit A (Light Rail) (in)	Transit B (Heavy Rail) (in)	Transit C (Heavy Rail) (in)
Track gage	56.75	56.5	56.5
Back-to-back distance	54.19	53.31	53.38
Flange thickness	1.12	1.42	1.16
Flange front clearance	0.33	0.35	0.81
Flangeway width based on Guideline 1	0.85	1.17	1.37
Flangeway width based on Guideline 2	1.45	1.77	1.97
Design flangeway width	1.75	1.88	2
Flangeway width tolerance for maintenance	1.75~2	1.75~2.25	*

*No data available.

Wharton Diagram," a graphical method developed about 100 years ago. A modified version of the Filkins-Wharton Diagram, referred to as the Nytram Plot, was developed in for *TCRP Report 57* (*4*). Both methods use a graphical technique to visualize the W/R contact for proper gage and flangeway width; the Nytram Plot uses a contemporary computer-aided design (CAD) technique.

Wheel binding can occur when the flangeway width is small and the wheelset angle of attack (AOA) becomes large enough to cause contact to occur between the front of the flange and the back of the flange on the same wheel. Another form of binding can occur in double-guarded installations (guard/girder/restraining rail on both high and low rails) where back-of-flange contact occurs on both wheels. This form of binding can be caused by the back-to-back spacing of the wheels being incompatible with the positions of the guard/girder/restraining rail. Large wheelset AOA increases this binding effect.

The geometric analysis is useful in determining the minimum gage and flangeway width for guard/restraining rail design to avoid wheel binding or wheel double flanging (which occurs when there isn't enough W/R clearance). However, the geometric analysis can't take into account dynamic factors such as the W/R friction coefficients. Geometric analysis also can't provide dynamics information such as W/R interaction forces and wear. The optimal gage and flangeway width have to be determined through W/R dynamic analysis based on W/R forces and wear, which are primary concerns to most transit systems.

2.4 Guard/Restraining Rail Height

The guideline for guard/restraining rail installation height in *U.S. Transit Track Restraining Rail—Volume II: Guidelines* (*3*) is quoted below:

> The top of the restraining rail should be between 0.25 and 0.5 in. above the track surface of the low rail. Additional height is desirable if feasible, for it will place the bottom of the guard face above the low point of the flange, so that undesirable "step" wear will not occur.

Table 3 shows that transit systems use different standards.

The guideline indicates that it is desirable to install the restraining rail as high as possible above the low rail. The unique conditions of flange back contact, however, require consideration of some three-dimensional features. As Figure 6 shows, the longitudinal shift (L) of the contact point on the flange back can be calculated by Equation 1, which has been previously used in a steady state curving model to simulate the effects of restraining rails on vehicle performance under steady state curving conditions (*5, 6, 7*).

$$L = \sqrt{R_2^2 - (R_1 - H)^2} \tag{1}$$

where

R_1 = the rolling radius of the contact point on the wheel tread,
R_2 = the wheel back of the flange contact circle radius, and
H = the height of the running rail.

Equation 1 shows that the higher the restraining rail is above the running rail (H), the larger the longitudinal shift (L). There is also an inward shift (v) in the lateral contact point between the flange back and the guard rail due to the wheelset yaw angle (ψ), which can be calculated using Equation 2:

$$v = L\sin(\psi) \tag{2}$$

Larger longitudinal shifts produce larger lateral contact shifts. Higher restraining rails cause larger longitudinal shifts, resulting in a need for greater flangeway width to accommodate the inward shift of the flange back contact point. Based on this analysis,

Table 3 Guard/restraining rail heights in three transit systems

Geometry Parameters	Transit A (Light Rail) (in)	Transit B (Heavy Rail) (in)	Transit C (Heavy Rail) (in)
Restraining rail height	*	1/16~1	1/16
Low rail top wear limit	1/2	Average 1/2, maximum 5/8	5/8

*No data available.

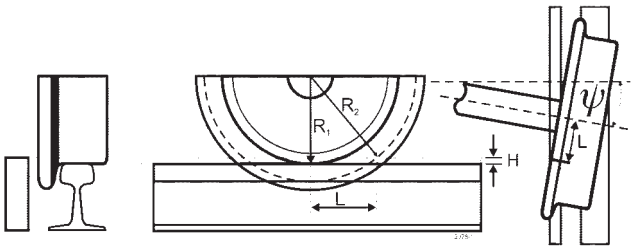

Figure 6 W/R contact geometry in two point flange back contact.

the installation height of the restraining rail should also take into account the optimization of flangeway width.

2.5 Rail Lubrication

It is a common practice for transit systems to lubricate rails or apply other friction modifiers. Various types of lubricants and lubricators have been used by transit systems; however, the lubrication effect is influenced by many factors and no general specifications have been developed (*8*). The effect of lubrication on low rails, high rails, and restraining rails needs to be further investigated to minimize system wear.

2.6 Summary of the Survey

The survey shows that transit systems use different restraining rail designs and maintenance standards based on their individual tracks, vehicle characteristics, and practical experience. Some of the current guidelines are not supported by current practices, and a detailed study to develop general restraining rail guidelines is needed for transit systems. Once the general guidelines are developed, they can be targeted to meet specific design and maintenance standards for individual transit systems.

The guard/girder/restraining rail geometric dimensions and parameters have important effects on W/R interaction. The geometric analysis is the basic method used for guard/restraining rail design; however, the optimization of design parameters needs to be determined through W/R dynamic analysis to account for W/R forces and wear, which are primary concerns to most transit systems.

The following sections describe the effect of guard/girder/restraining rail geometric parameters including flangeway width and height, track gage, track curvature, wheelset AOA, W/R profile shapes, and lubrications on the W/R forces and wear as determined through NUCARS® simulations. Based on these analyses, preliminary guidelines for optimized guard/girder/restraining rail design have been proposed.

3 THREE-DIMENSIONAL W/R CONTACT GEOMETRY

A W/R contact model and contact geometry are the core elements of any railway vehicle dynamics simulation. Most simulation software packages, including the standard rigid W/R contact model versions of NUCARS®, assume that the wheel and rail are two-dimensional objects for the application of most railroad dynamics simulations. This assumption permits the contact geometry calculations to be performed more easily than they could be if the actual three-dimensional geometry of the wheels and rails were considered. A result of the assumption that the wheel and rail are two-dimensional objects is that the contact geometry table generated by the software is independent of the wheelset yaw angle, or AOA, relative to the rails. This makes the table size smaller and interpolation more efficient.

In reality, however, the contact geometry characteristics are functions of wheelset AOA. For most railroad applications, simulations using the two-dimensional W/R contact assumption produce sufficiently accurate results because small radius curves are uncommon. Correspondingly, the wheelset AOA is relatively small. However, the three-dimensional contact effect is significant, especially for guard/girder/restraining applications on sharp curves where transit vehicle wheelset AOAs are much larger than those generated under typical railroad operation conditions.

To describe the wheel and rail shapes and contact geometry, two coordinate systems are used by NUCARS®. Figure 7 shows the wheelset reference frame X, Y, Z and the track reference frame XR, YR, ZR. Both coordinate systems follow the right hand rules. The wheelset yaw angle is relative to the track reference frame. Wheelset yaw angle or AOA is usually measured in milliradians (mrad). One mrad is approximately equal to 0.0573 degrees.

3.1 Wheel with a 75-Degree Flange Angle

The W/R contact geometry for a transit vehicle wheel with a 75-degree flange angle is investigated in this section. Figure 8 shows the projection of the

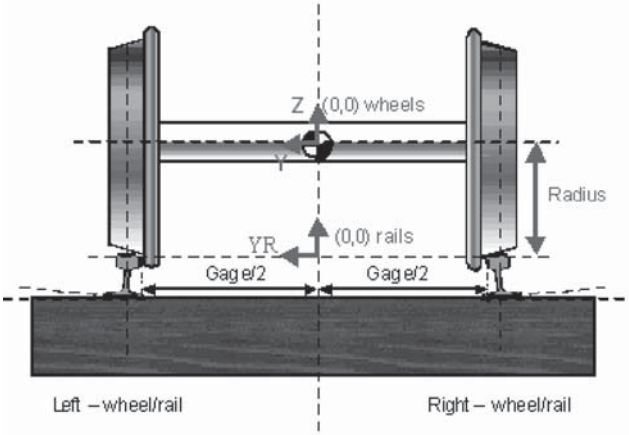

Figure 7 NUCARS® wheel (AOA = 0 mrad) and rail reference frames.

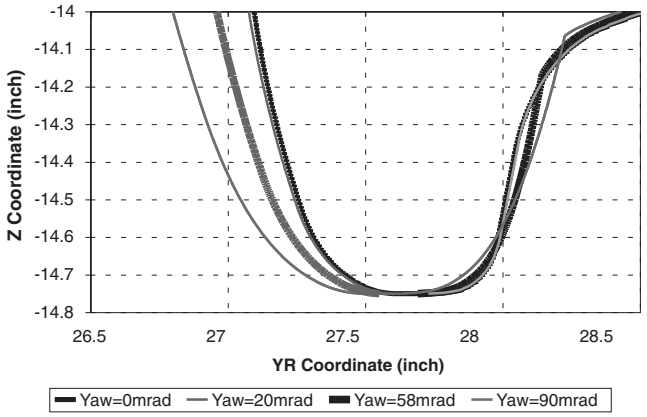

Figure 9 Close-up view of wheel flange projection on XR = 100-in. plane.

right wheel with different yaw angles onto the rail, XR = 100-in. plane. These wheel profiles are the wheel contour as observed in the track reference.

Figure 9 shows a close-up view of the flange projection. Figures 8 and 9 clearly show that the projection of the wheel contour changes with yaw angle; the wheel flange contour changes very little when the yaw angle is less than 20 mrad. The wheel contour when the yaw angle is zero is used for the two-dimensional W/R contact model.

Because the wheel contour difference between the two-dimensional and three-dimensional contact model is small when the yaw angle is less than 20 mrad, the two-dimensional W/R contact model is acceptable for W/R dynamics simulations in which wheelset yaw angles are less than 20 mrad, such as curving simulations for curve radii greater than 290 ft (20 degrees curvature).

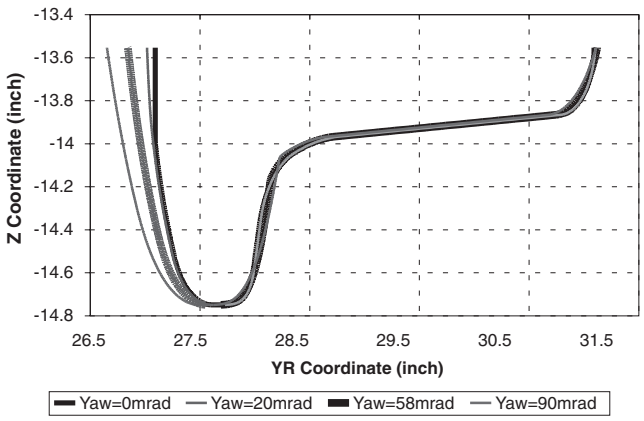

Figure 8 Wheel projection with different yaw angle on XR = 100-in. plane.

As Figures 8 and 9 show, the three-dimensional wheel flange contour changes dramatically when the yaw angle is greater than 20 mrad. The distance between the wheel flange back and the maximum flange angle contour line becomes wider as the yaw angle increases; some transit experts refer to this widening as the flange "fattening" effect of three-dimensional W/R contact.

Because of flange fattening, W/R clearance decreases with the increasing yaw angle. In order to keep enough W/R clearance for the wheel to go through curves freely, transit systems commonly increase the gage on sharp curves.

As Figure 9 shows, the flange contour thickness at a yaw angle of 58 mrad increases about 0.2 in. compared with the two-dimensional flange shape. For this example, the thickness increase is close to the flangeway width maintenance limit (about 0.25 in.) and gage increase value (0.25 in. and 0.125 in. on each side); therefore, the three-dimensional contact effect is significant for a typical guard/girder/restraining rail design.

For sharp curves (100-ft radius), the wheelset yaw angle could be larger than 58 mrad, and the two-dimensional W/R contact model would lead to incorrect conclusions, as shown in Section 4.5.1. The three-dimensional W/R contact model is therefore necessary for accurate dynamics simulations of railway vehicles negotiating sharp curves, especially when there is W/R contact on the wheel flange back or wheel back.

For the two-dimensional W/R contact model, the wheel contour at a yaw angle of zero is used for the W/R contact geometry calculation and never changes with wheelset yaw angle in the simulation.

For the three-dimensional contact model, the three-dimensional wheel contour for different yaw angles must be generated before performing the simulation. Even though the wheel contour is not changed with the wheelset yaw angle during the simulation, the longitudinal shift of the contact point on the wheel caused by the yaw angle is calculated based on a simplified three-dimensional contact algorithm in NUCARS® for both the two-dimensional and three-dimensional W/R contact models (*7*).

Another difference between three-dimensional and two-dimensional contact models is found in the maximum W/R contact angle, as Figure 10 shows. The maximum W/R contact angle relative to the track frame is 75.29 degrees for the two-dimensional contact model. For the three-dimensional contact model for a wheelset with a yaw angle of 58 mrad, the maximum W/R contact angle relative to the track frame is 74.12 degrees. Because the wheel lateral-to-vertical (L/V) ratio limit (Nadal value) is determined by the maximum contact angle, simulation results using the two-dimensional contact model instead of the three-dimensional contact model are not conservative for predictions of L/V ratios for railway vehicles negotiating sharp curves.

The W/R clearance predicted by the three-dimensional contact model for a wheelset with a yaw angle of 58 mrad is about 0.05 in. smaller than the W/R clearance predicted by the two-dimensional contact model, as Figure 10 shows.

3.2 Wheel with a 63-Degree Flange Angle

Figure 11 shows the three-dimensional W/R contact model projection for a wheel with a 63-degree flange angle at a yaw angle of 0 mrad and a yaw angle of 58 mrad.

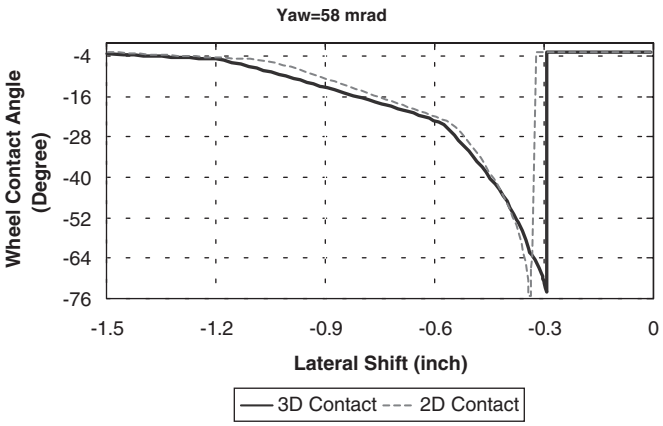

Figure 10 W/R contact angles for two-dimensional and three-dimensional contact models.

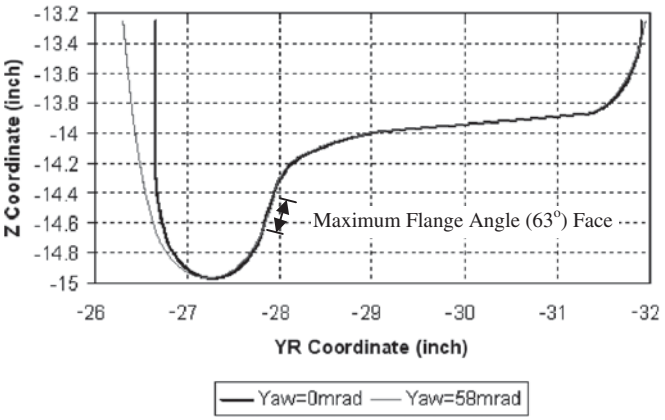

Figure 11 Projection of wheel body with 63-degree flange angle on XR = 100-in. plane.

As Figure 11 shows, the wheel contour on the maximum flange angle portion of the wheel at a yaw angle of 58 mrad is very close to the two-dimensional flange shape, which is different from the situation for a wheel with a 75-degree flange angle. Because the fattening effect on the maximum flange angle portion of the wheel is negligible, the W/R clearance change is also negligible. So, there is no need to worry about the narrowing of W/R clearance, and hence no need to increase gage on sharp curves for wheelsets with flange angles less than 63 degrees, from the point of view of W/R geometry.

Even though the fattening effect on the 63-degree maximum flange angle portion of the wheel is negligible, the fattening effect on the wheel flange back and wheel back is as significant as that of the wheel with a 75-degree flange angle. To allow enough clearance for wheels to negotiate curves, increasing flangeway width makes more sense than increasing gage if a guard/girder/restraining rail is installed.

4 GUARD/GIRDER/RESTRAINING RAIL PARAMETER OPTIMIZATION

A centrifugal force acts on a rail vehicle as it negotiates a curve. Superelevation of the high rail causes gravity to provide part of the force to react to the centrifugal force. The uncompensated centrifugal force on a vehicle as it negotiates a curve has to be balanced by the W/R forces. The high rail bears larger lateral forces than the low rail because of the action of the unbalanced centrifugal force and lateral creep forces caused by axle AOA. The guard rail

can't decrease the lateral force on an axle; however, the distribution of the lateral W/R forces between high rail and guard rail can be controlled by the guard rail installation position. W/R wear can also be controlled by the guard rail installation position because it is proportional to W/R forces. An optimization methodology based on W/R lateral forces and wear is described in this section.

4.1 Optimization Objective Functions: W/R Interaction Forces and Wear

It is widely accepted that W/R wear can be evaluated in terms of a wear index. In NUCARS®, the wear index is calculated as the sum of the tangential forces (T_x, T_y, and M_z) multiplied by the creepages (γ_x, γ_y, and ω_z) at the contact patch, as Equation 3 shows. A higher wear index can induce either rolling contact fatigue or higher rates of wear.

$$\text{Wear Index} = \sum_n T_x\gamma_x + T_y\gamma_y + M_z\omega_z \quad (3)$$

The sum of the wear indices of all wheels is defined as the vehicle rolling resistance in NUCARS®. As its name implies, vehicle rolling resistance is also a key indicator of the energy consumption at the W/R interface. The wear index can also be seen as a measure of the drag induced in the contact patch. The total rolling resistance of the vehicle due to wheel rail contact is obtained by summing the wear indices for all W/R contact points on a vehicle.

The W/R lateral forces, wear index, or rolling resistance are the objective functions for guard rail parameter optimization. The optimization objectives are the following:

- To mitigate excessive W/R lateral forces and wear on the high rail or the guard rail and
- To make the high rail and guard rail wear at the same rate.

The benefits of installing optimized guard rails are the following:

- Decreasing track component damage and irregularities by mitigating the excessive W/R lateral forces and wear and
- Decreasing rail renewal frequency and cost by distributing the W/R lateral forces and wear equally between the high rail and the guard/restraining rail.

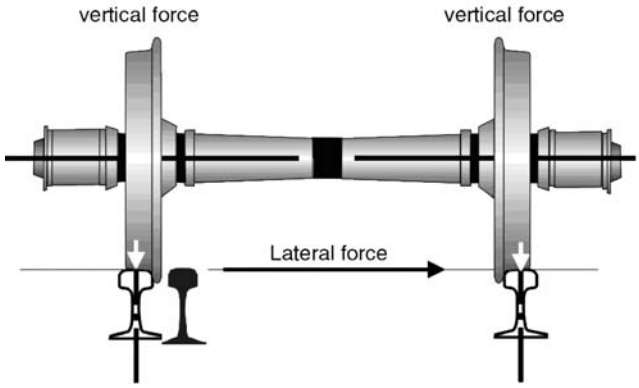

Figure 12 Single wheelset flange climb model.

4.2 Single Wheelset Simulation Model

Figure 12 shows a simple single wheelset flange climb model with guard/restraining rail installed on the low rail that was used in the simulations to investigate the effects of various factors on W/R forces and wear. Large yaw stiffness between the axle and ground ensured that the AOA remained approximately constant throughout the flange climb process.

A vertical wheel load corresponding to a typical transit vehicle axle load was applied to the wheelset to obtain the appropriate loading at the wheel/rail contact points.

To make the right wheel climb on the high rail and the left wheel contact on the guard/girder/restraining rail, an external lateral force was applied to the derailing wheel at the height of the rail head and acting toward the field side of the derailing wheel. Figure 13 shows the lateral force distance history. During a constant speed movement, the lateral force was applied on the wheel in three steps for steady-state climb and was held until the end of the simulation. The right wheel either climbed on top of the right rail to derail, or reached an equilibrium state with the left wheel contacting the guard/girder/restraining rail.

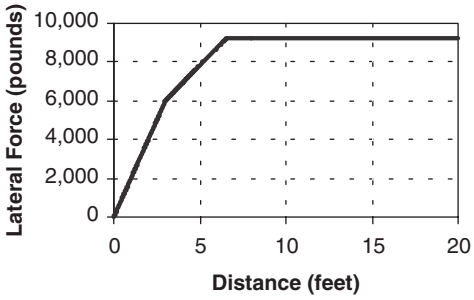

Figure 13 Lateral force step input.

Table 4 W/R parameters for guard rail simulations

Parameters	Value
Wheel back-to-back distance	54.1875 in
Wheel maximum angle	75 deg
Wheel nominal radius	14 in
Running rail	AREMA 115-lb rail
Guard rail height	0.1 in above low rail top
Gage	56.75 in
Wheelset AOA	20 mrad
W/R friction coefficients	Guard Rail 0.3, Running rail 0.5

4.3 Guard Rail

In this section, the results of NUCARS® simulations to investigate the effect of various guard rail parameters on the W/R lateral forces are discussed.

4.3.1 Effect of Flangeway Width

Table 4 lists the basic W/R parameters used for guard rail simulations.

The flangeway width has the most important effect on W/R forces and wear. As Figure 14 shows, for a 75-degree flange angle wheel with a 20-mrad yaw angle, if the flangeway width is too narrow (less than or equal to 1.5 in.), the guard rail bears almost all the lateral force; there is no lateral force acting on the high rail (right rail). Correspondingly, the left wheel wears severely on the guard rail, but the right wheel wear index is relatively small on the high-rail tread and flange, as Figure 15 shows. The guard rail and fastener components could be damaged because of the high lateral force and the guard rail service life could also be reduced by severe wear.

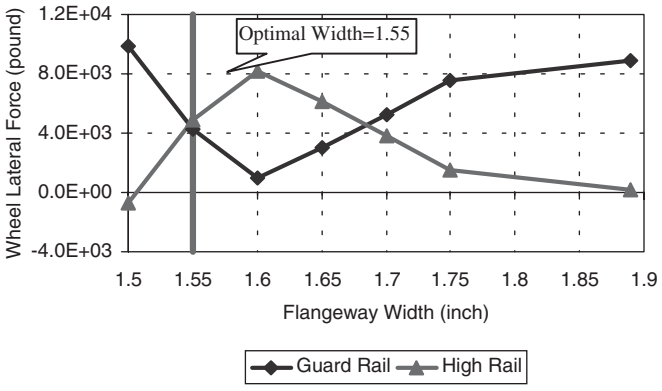

Figure 14 Guard rail W/R lateral forces, wheel flange angle = 75 degrees, AOA = 20 mrad.

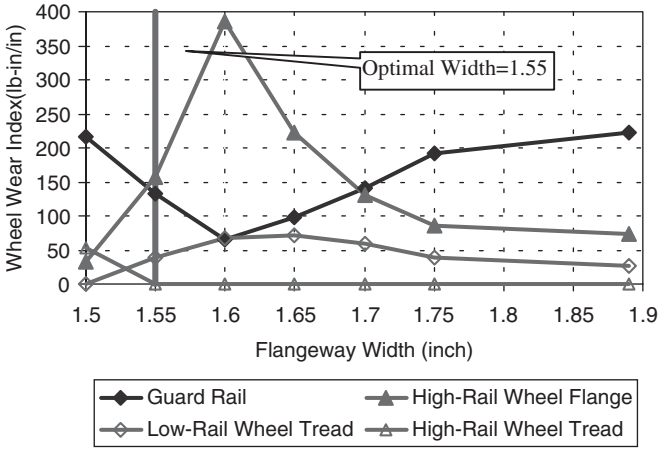

Figure 15 Guard rail W/R wear, wheel flange angle = 75 degrees, AOA = 20 mrad.

In NUCARS®, W/R interaction can be visualized through animation. The narrow flangeway width leads to flange back climb onto the guard rail, as Figure 16 (a) shows. In the animation pictures, the lines perpendicular to the W/R profiles indicate the W/R contact point positions. Even though the right rail contact helps to reduce flange back climb derailment risk, the flange back climbing on top of the guard rail should be avoided.

As the flangeway width increases to 1.55 in., the left and right W/R contact points share the total lateral force equally, and the guard rail and high-rail gage face also wear equally, as Figures 14 and 15 show. The balance of lateral W/R forces and wear between the high rail and the guard rail meet the optimization objectives stated in Section 4.1. The 1.55-in. flangeway width is the optimal value for the cases with the W/R parameters listed in Table 4.

Figure 16 (c) shows that as the flangeway width increases to 1.60 in., the right wheel maximum flange angle partly contacts on the high rail, while the left wheel flange back contacts on the guard rail at the same time. The right wheel wears severely because of the high contact angle and bears most of the lateral force (as Figures 14 and 15 show). Clearly, the high rail wears faster, resulting in a shorter service life.

Figure 16 (d) shows that as the flangeway width increases to 1.70 in., the right wheel flange tip contacts on the high rail, while the left wheel flange

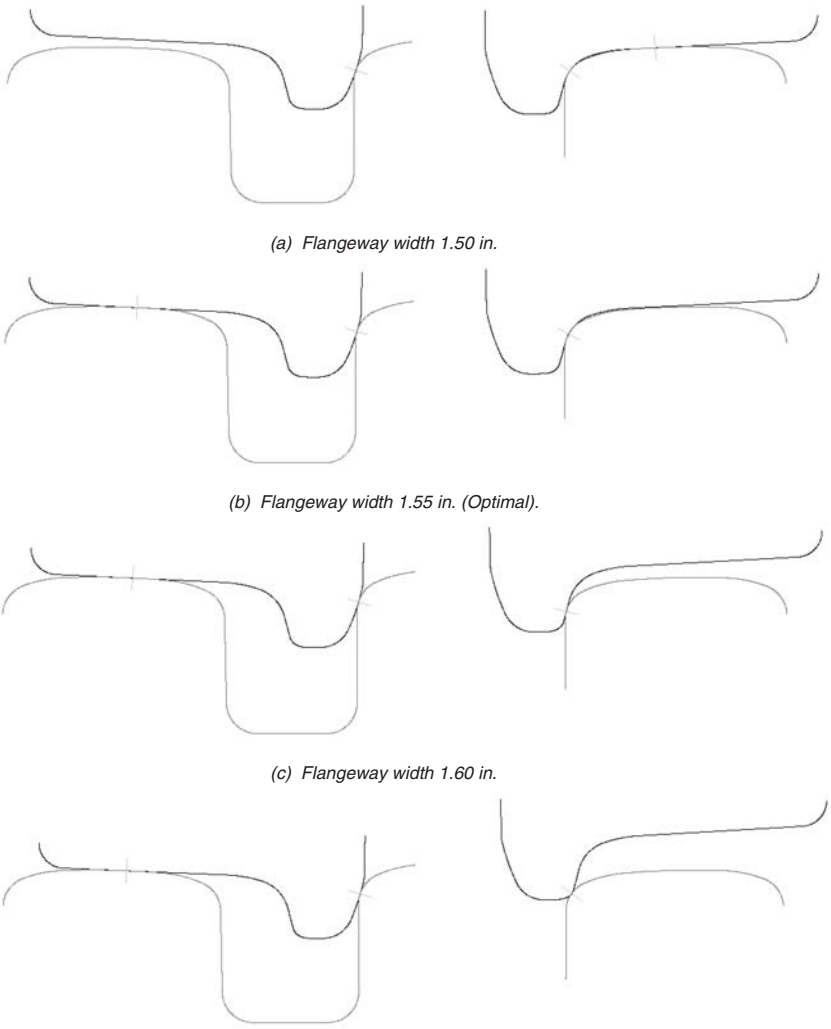

(a) Flangeway width 1.50 in.

(b) Flangeway width 1.55 in. (Optimal).

(c) Flangeway width 1.60 in.

(d) Flangeway width 1.70 in.

Figure 16 Guard rail W/R contact animation, wheel flange angle = 75 degrees, AOA = 20 mrad.

back contacts on the guard rail at the same time. Even though the lateral forces and wear are almost in balance between the high rail and guard rail (as Figures 14 and 15 show), the 1.70-in. flangeway width is not the optimal value because of the high derailment risk created by these W/R contact conditions. To understand the derailment mechanism caused by these W/R contact conditions, the lateral creep force effect on flange climb derailment has to be examined.

Figure 17 shows the forces acting on a wheel. A friction angle, β, corresponding to the W/R friction coefficient, μ, can be defined as in Equation 4:

$$\beta = \tan^{-1} \mu \quad (4)$$

Assuming the W/R friction coefficient is 0.5 for normal W/R conditions, the friction angle is calculated as 26.6 degrees.

Figure 17 shows the wheel flange tip in contact with the rail at a 26.6-degree angle. Between the maximum contact angle (*Q*) and the 26.6-degree flange tip angle (*O*), the wheelset can slip back down the gage face of the rail because of its own applied vertical load (*V*) if the external lateral force (*L*) is suddenly reduced to zero. In this condition, the lateral creep force, *F,* (caused by AOA) by itself is not large enough to cause the wheel to derail.

When the wheel climbs past the 26.6-degree contact angle (*O*) on the flange tip, the wheelset cannot slip back down the gage face of the rail because of its

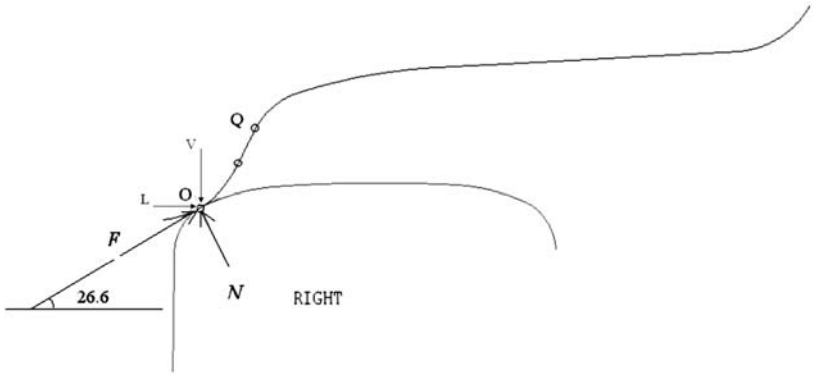

Figure 17 Wheel/rail interaction and contact forces on flange tip.

own applied vertical load. The lateral creep force, *F,* generated by the wheelset AOA is large enough to resist the fall of the wheel and forces the flange tip to climb on top of the rail.

If there is a guard rail on the low rail, the right wheel can neither climb further up to the high-rail top because of the guard rail protection, nor slip back to tread contact because the creep force is large enough to resist wheel slip when the flange tip contact angle is smaller than the friction angle. The locked right wheel could easily derail under small perturbations when the wheelset exits the curve protection.

The above analyses show that a narrow flangeway width leads to early W/R contact and wheel flange back climb onto the guard rail and a wide flangeway width leads to wheel flange climb on the high rail. A reasonable flangeway width makes the front W/R clearance between the wheel flange face and the high rail equal to the back clearance between the wheel flange back and the guard rail. However, the optimal flangeway width depends not only on the W/R contact geometry, but also on parameters such as the W/R friction coefficients (as discussed in Section 4.3.5).

4.3.2 Effects of Axle AOA and Track Curvature

The wheelset AOA increases with increasing track curvature. A previous study showed that the leading wheelset AOA in mrad is approximately equal to the curvature in degrees for most truck configurations (*1*). This assumption is validated through vehicle simulation in Section 5. Based on this assumption, the 12-, 20-, and 58-mrad wheelset AOAs correspond approximately to a wheelset negotiating a curve with 500-, 290-, and 100-ft radii, respectively. The track gage for a 20-degree curve (290-ft radius) is 56.75 in., 0.25 in. wider than the standard gage.

Figures 18 and 19 show the W/R forces and wear indices for a wheelset with a 12-mrad AOA and the other parameters listed in Table 4.

The optimal flangeway width for a 12-mrad AOA is 1.55 in., the same width as for a 20-mrad AOA, because the three-dimensional wheel contour variation is negligible for a wheelset with an AOA smaller than 20 mrad.

Figures 20 and 21 show the W/R forces and wear indices for a wheelset with a 58-mrad AOA, a three-dimensional contact wheel contour, and the other parameters listed in Table 4. The optimal flangeway width for a wheelset with a 58-mrad AOA is about 1.62 in., 0.07 in. wider than the optimal flangeway width of the 20-mrad AOA case because of the three-dimensional contact wheel flange fattening effect at higher AOA (larger than 20 mrad).

For axle AOA higher than 20 mrad, the optimal flangeway width should increase with increasing

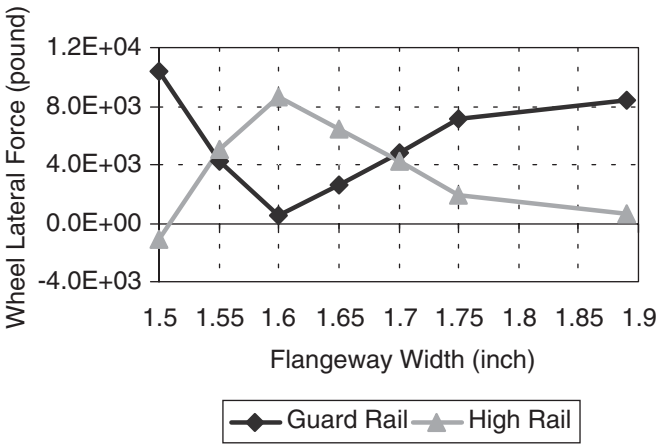

Figure 18 Guard rail W/R lateral forces, wheel flange angle = 75 degrees, AOA = 12 mrad.

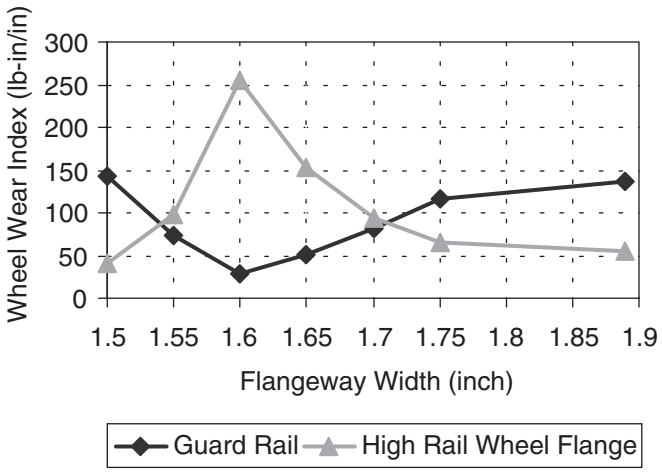

Figure 19 Guard rail W/R wear, wheel flange angle = 75 degrees, AOA = 12 mrad.

AOA/track curvature if the three-dimensional flange back fattening effect is larger than that on the max flange angle face (this situation applies to most W/R contact cases).

4.3.3 Effect of Gage

It is a common practice for transit systems to increase gage on sharp curves. Figures 22 and 23 show the W/R forces and wear indices for a wheelset with a 58-mrad AOA, a 0.25-in. gage increase (57-in. gage), and the other parameters listed in Table 4. For the 1.625-in. flangeway width case, the high-rail and low-rail wheel lateral forces are in balance, but the right wheel wear index on the high rail is three times

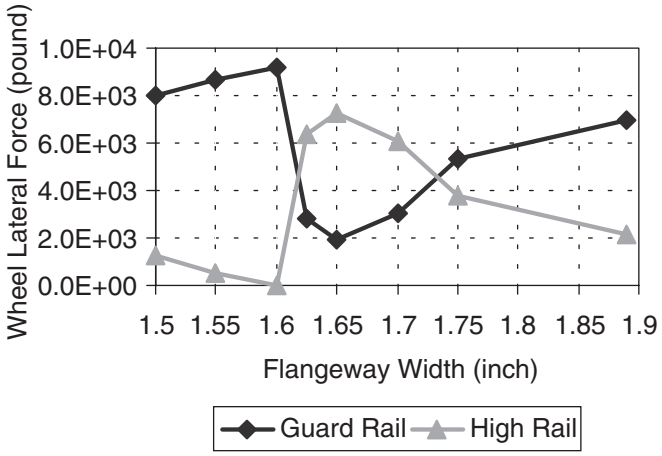

Figure 20 Guard rail W/R lateral forces, wheel flange angle = 75 degrees, AOA = 58 mrad.

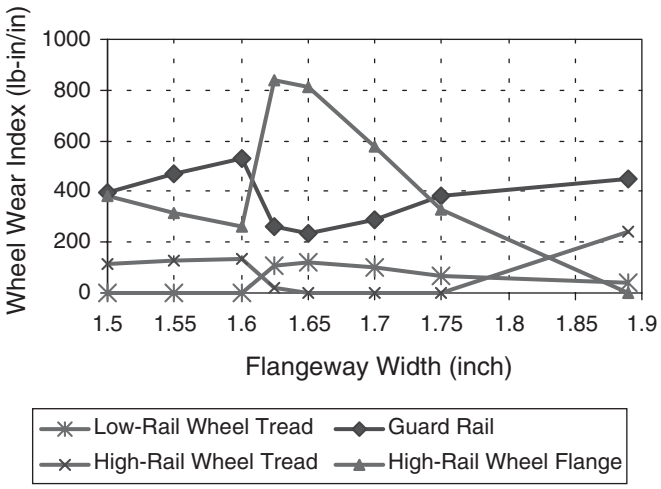

Figure 21 Guard rail W/R wear, wheel flange angle = 75 degrees, AOA = 58 mrad.

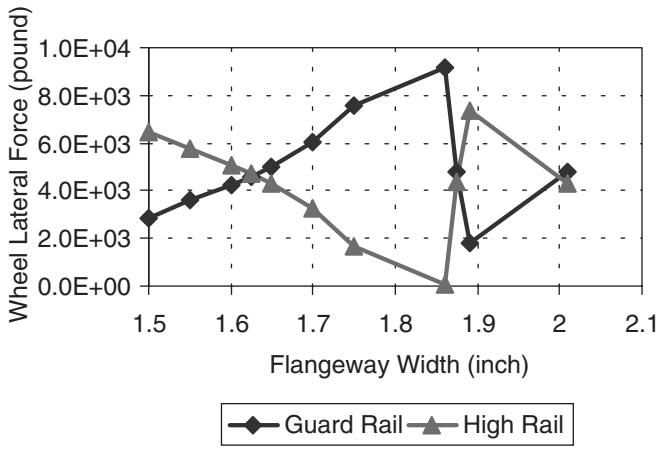

Figure 22 Guard rail W/R lateral forces, wheel flange angle = 75 degrees, AOA = 58 mrad, gage = 57 in.

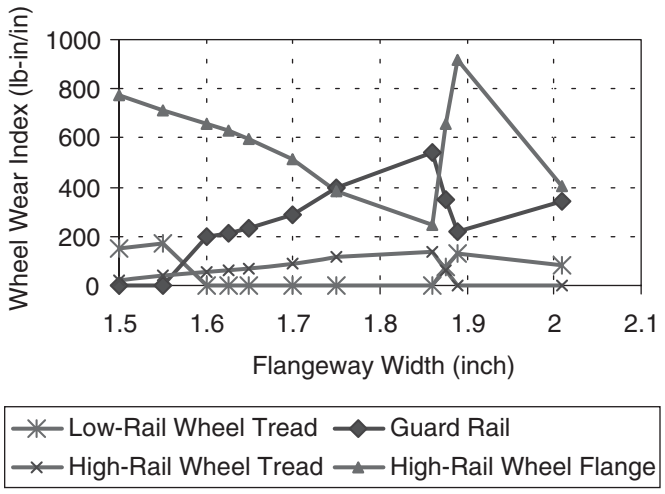

Figure 23 Guard rail W/R wear, wheel flange angle = 75 degrees, AOA = 58 mrad, gage = 57 in.

higher than that of the left wheel, which climbs onto the guard rail at the flange tip, as Figure 24 (a) shows. The optimal flangeway width for the 58-mrad AOA with 0.25-in. gage increase is about 1.87 in., 0.25 in. wider than without the gage increase. Figure 24 (b) shows the contact situation. The wide flangeway width, as Figure 24 (c) shows, leads to the increased risk of flange climb on the high rail (as discussed in Section 4.3.1).

Clearly, increasing gage without increasing flangeway width leads to early contact of the left wheel flange back on the guard rail and higher lateral forces and wear. To avoid early contact, the flangeway width has to be increased to correspond with the gage increase.

Increasing gage or decreasing flangeway width leads to a tendency of increasing lateral W/R forces and wear on guard/girder/restraining rails because increasing gage increases the W/R flange front clearance and decreasing flangeway width decreases the flange back clearance. Both of these effects cause the guard/girder/restraining rail to contact the wheelset before the high rail contacts the flange face. Correspondingly, decreasing gage or increasing flangeway width leads to a tendency of increasing lateral W/R forces and wear on high rails.

4.3.4 Effect of Guard Rail Height

Figure 25 shows the W/R forces and wear indices for a wheelset with a guard rail 0.2 in. above the running rail and the parameters listed in Table 4. The optimal flangeway width increases about 0.02 in. compared with the 1.55-in. optimal flangeway width for a guard rail 0.1 in. above the running rail.

Figure 26 shows that the optimal flangeway width increases to 1.6 in. as the guard rail height increases to 0.3 in. above the running rail.

Because the contact point height on the left wheel flange back increases with increasing guard rail

(a) Flangeway width 1.625 in.

(b) Flangeway width 1.875 in.

(c) Flangeway width 2.01 in.

Figure 24 Guard rail W/R contact animation, wheel flange angle = 75 degrees, AOA = 20 mrad, gage = 57 in.

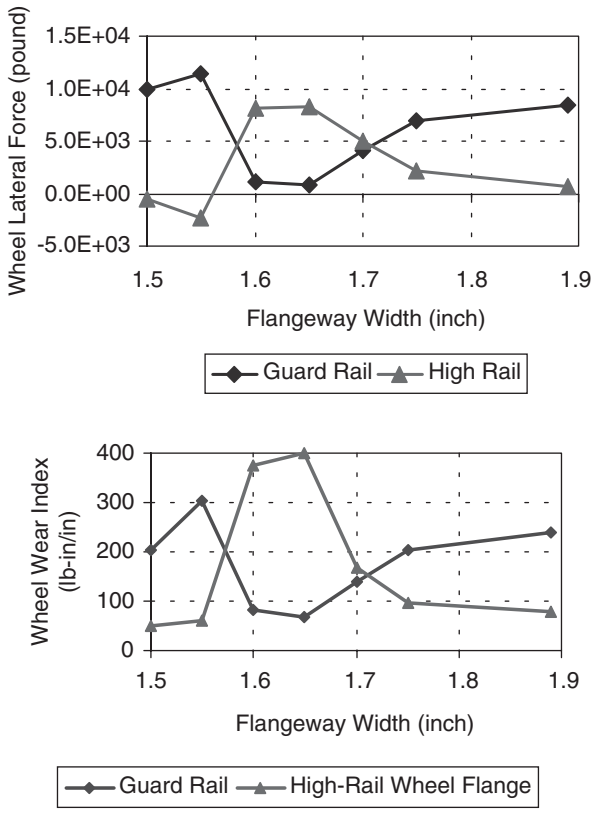

Figure 25 Guard rail W/R lateral forces and wear, wheel flange angle = 75 degrees, AOA = 20 mrad, guard rail height = 0.2 in.

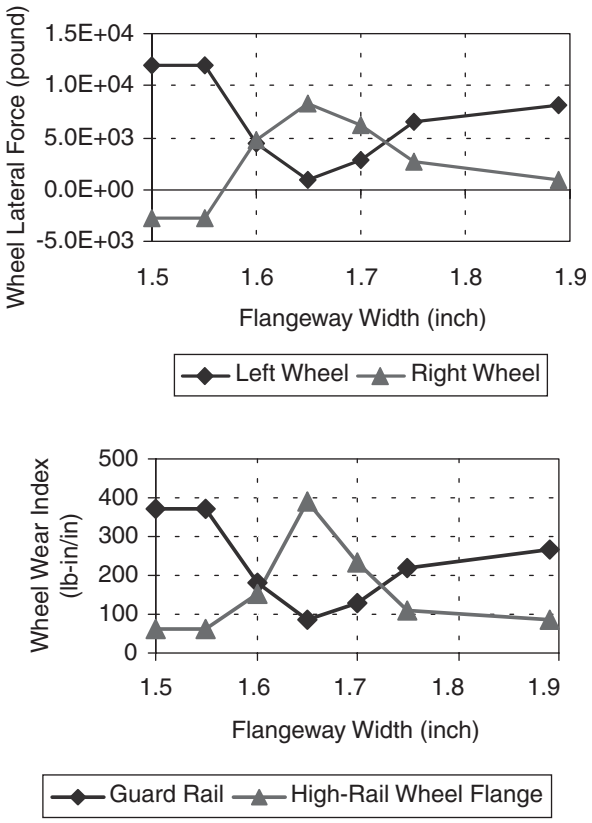

Figure 26 Guard rail W/R lateral forces and wear, wheel flange angle = 75 degrees, AOA = 20 mrad, guard rail height = 0.3 in.

height, the clearance between the wheel flange back and guard rail decreases. Correspondingly, the optimal flangeway width has to increase to keep the same flange front clearance and flange back clearance.

In general, rolling resistance increases with increasing guard rail height, as Figure 27 shows. However, the guard rail height effect on the maximum rolling resistance and resistance at optimal flangeway width is relatively small.

4.3.5 Effect of Guard Rail Lubrication

Figure 28 shows rolling resistance with different guard rail lubrication conditions. Clearly, rolling resistance increases with increases in the W/R friction coefficient (mu). In Figure 28, the label "Flanging, Guard mu 0.1" means that the friction coefficient on both the flanging wheel and the guard rails is 0.1; the mu for other labels refers only to the friction coefficients on guard rails.

As figure 28 shows, the rolling resistance decreases dramatically when both the high-rail wheel flange and the guard rail are lubricated to 0.1 friction coefficient.

However, the low rolling resistance values can't guarantee that the optimization objectives listed in Section 4.1 will be reached. The following example shows that improper lubrication on the guard rail can

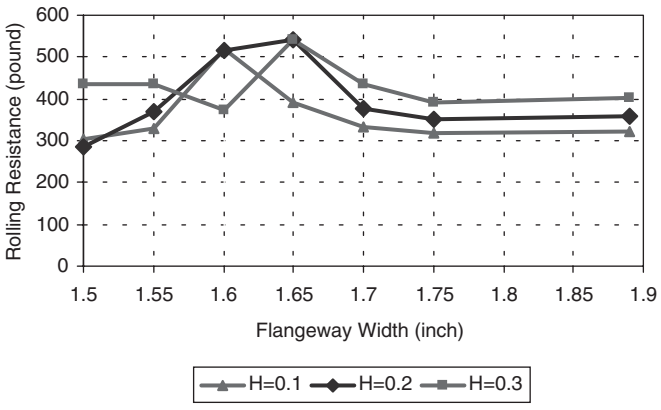

Figure 27 Effect of guard rail height on rolling resistance.

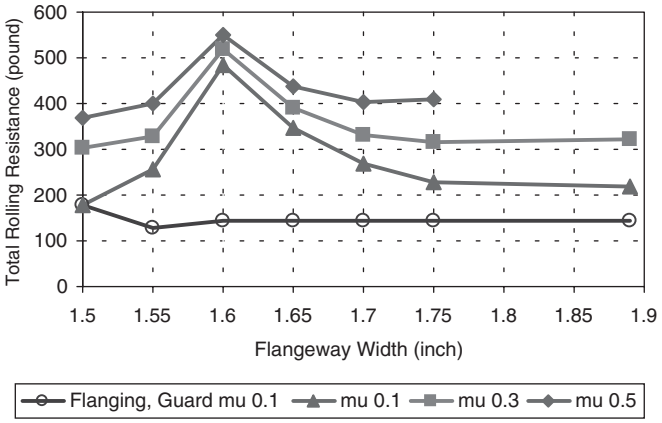

Figure 28 Effect of guard rail lubrications on rolling resistances.

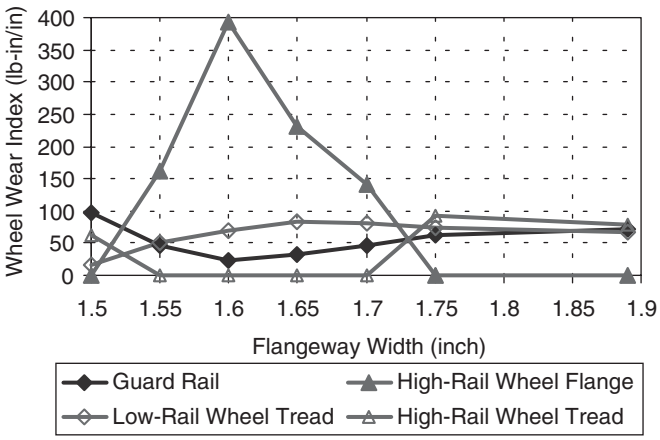

Figure 30 Guard rail W/R wear, wheel flange angle = 75 degrees, AOA = 20 mrad, guard rail mu = 0.1.

lead to unbalanced wear between the high rail and low rail.

Figures 29 and 30 show the W/R forces and wear indices for a wheelset with a 0.1 friction coefficient on the guard rail and the parameters listed in Table 4. As Figures 29 and 30 show, for a guard rail with a 1.55-in. flangeway width, the high rail and guard rail share the lateral load equally; however, the high-rail wear index is three times higher than the wear index of the guard rail. The high wear index of the high rail increases the frequency of high-rail renewal and therefore increases costs. For a guard rail with a 1.525-in. flangeway width, the high-rail wear index is approximately equal to the wear index of the guard rail; however, the guard rail bears almost the entire lateral load, which leads to guard rail and fastening component damage at high lateral loads. So, for the case of heavy lubrication on the guard rail (guard rail mu = 0.1) and no lubrication on the high rail (high-rail flange mu = 0.5), a compromise 1.537-in. flangeway width could be a better choice than an optimal flangeway width. The best compromise value would have to be determined by comparing the cost of replacing the worn rail with the cost of damage to the fastening components and guard rail.

For cases of lubrication with 0.1 friction coefficients on both the guard rail and the high rail, the 1.55-in. flangeway width is not the optimal value; however, it is acceptable because the high-rail wear index equals that of the low-rail wear index (although the high rail bears more lateral force than the guard rail, as Figures 31 and 32 show). Because of the lubrication on the high rail, the right wheel contacts on the high rail with the maximum flange angle and

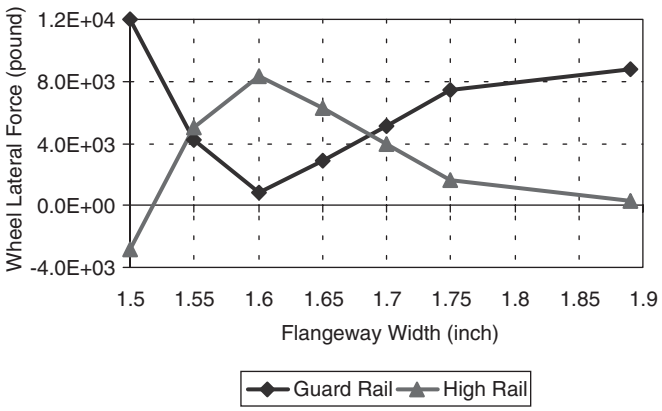

Figure 29 Guard rail W/R lateral forces, wheel flange angle = 75 degrees, AOA = 20 mrad, guard rail mu = 0.1.

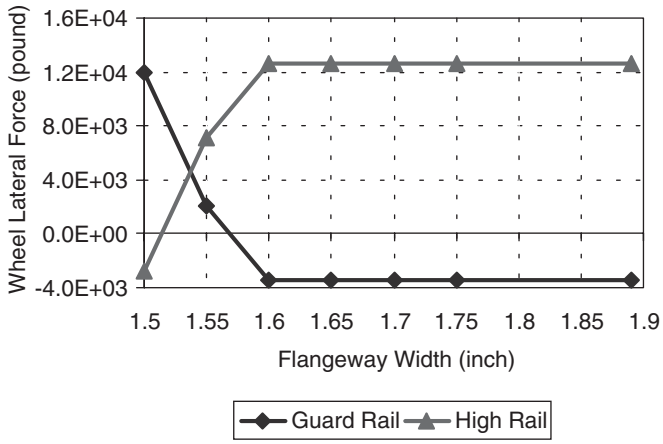

Figure 31 Guard rail W/R lateral forces, wheel flange angle = 75 degrees, AOA = 20 mrad, guard rail mu = 0.1, high-rail flange mu = 0.1.

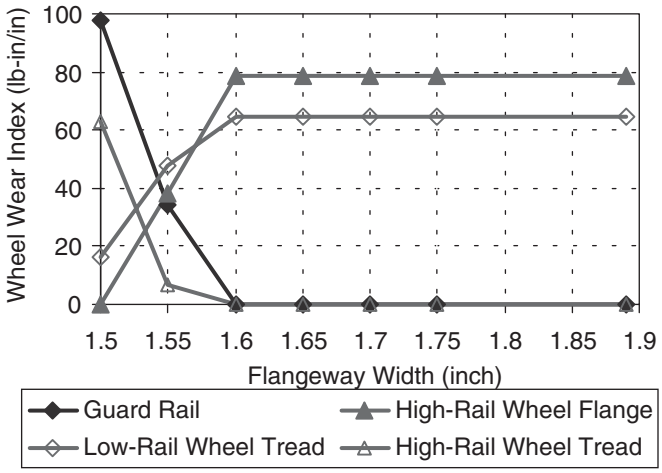

Figure 32 Guard rail W/R wear, wheel flange angle = 75 degrees, AOA = 20 mrad, guard rail mu = 0.1, high-rail flange mu = 0.1.

stops further climbing on the high rail under the lateral load that was shown in Figure 13; the left wheel doesn't contact the guard rail if the flangeway width is wider than 1.6 in., as Figure 33 shows.

For cases without lubrication (W/R friction coefficient mu = 0.5 for all contact points), the compromise flangeway width is about 1.56 in. because the high-rail wear index equals that of the low rail, although the high rail bears more lateral force than the guard rail, as Figures 34 and 35 show. The high W/R friction coefficients increase the flange climb derailment risk. As Figure 36 shows, for a guard rail with a 1.89-in. flangeway width, the right wheel climbs up to the high-rail top and the left wheel climbs up to the top of guard rail, and this situation ends with derailment. These simulation results indicate that excessive flangeway width can also lead to flange climb derailment under high W/R friction coefficients.

The above simulations show that the optimal flangeway width can only be obtained for the case with friction coefficients of 0.5 on the high rail and 0.3 on the guard rail; for other lubrication cases, the flangeway width has to be a compromise between the lateral forces and wear balance on the high rail and guard rail. The W/R contact angles for the case with the optimal flangeway width are 73.5 degrees on the guard rail and 61.7 degrees on the high rail, which implies that the optimal flangeway width design can be achieved through low friction coefficients on the high contact angle points and high coefficients on the low contact angle points. The approach for optimizing the flangeway width should also include a compatible lubrication methodology on the high rail and guard rail.

To verify this approach, a simulation case was conducted with friction coefficients of 0.3 on the high rail and 0.18 on the guard rail. Figures 37 and 38 show this approach is validated by the simulation results, which show that the optimal flangeway width is about 1.54 in. This approach can be used to generate

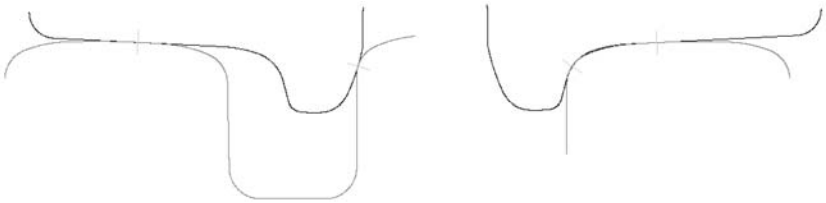

(a) Flangeway width 1.55 in.

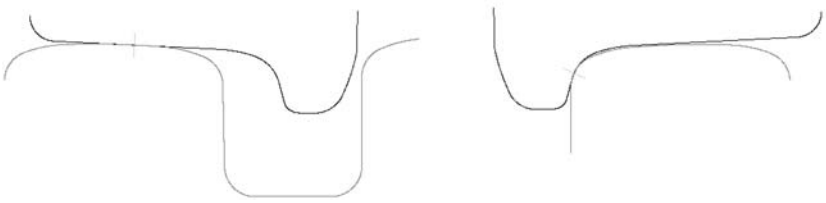

(b) Flangeway width 1.70 in.

Figure 33 Guard rail W/R contact animation with lubrication on guard rail and high-rail flange.

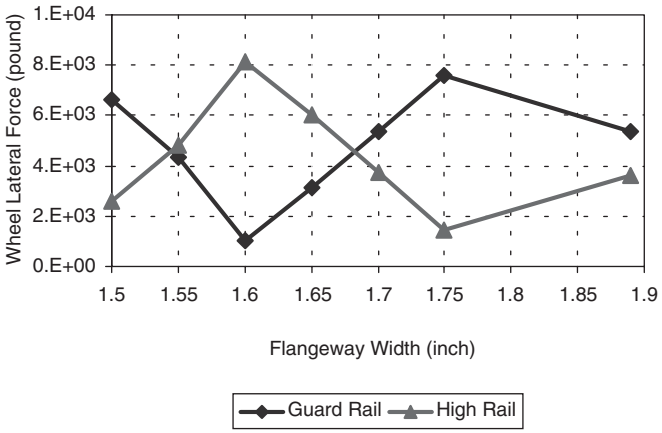

Figure 34 Guard rail W/R lateral forces, wheel flange angle = 75 degrees, AOA = 20 mrad (no lubrication), W/R friction coefficient mu = 0.5.

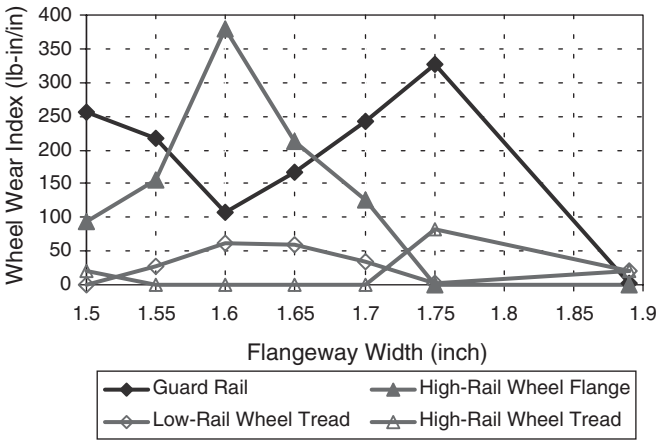

Figure 35 Guard rail W/R wear, wheel flange angle = 75 degrees, AOA = 20 mrad (no lubrication), W/R friction coefficient mu = 0.5.

guidelines for guard rail lubrication methodology in practice.

The following conclusions can be drawn from the guard rail simulations:

- The W/R contact geometry, including flange back contact and friction coefficients, has important effects on W/R forces and wear.
- The optimal flangeway width depends on wheel profile shape including flange back, wheel back-to-back distance, track gage, guard/girder/restraining rail profile shapes and installation height, and wheelset AOA or track curvature.
- The optimal guard rail installation, leading to balanced lateral W/R forces and wear between the high rail and the guard rail, can be achieved through control of the flangeway width and W/R friction coefficients.
- The optimal flangeway width makes the flange front W/R clearance between the wheel flange face and the high rail equal to the flange back clearance between the wheel flange back and the guard rail (see Figure 1).
- A wide flangeway width leads to high lateral forces and wear on the high rail and increases high-rail flange climb derailment risk.
- A narrow flangeway width leads to high lateral forces and wear on the guard rail and increases low-rail flange back climb derailment risk.
- The flangeway width should increase with wheelset AOA/track curvature for AOA larger than 20 mrad (corresponding to curves with about 290-ft radius) if the three-dimensional flange back fattening effect is larger than the fattening effect on the maximum flange angle face (this situation applies to most W/R contact cases).

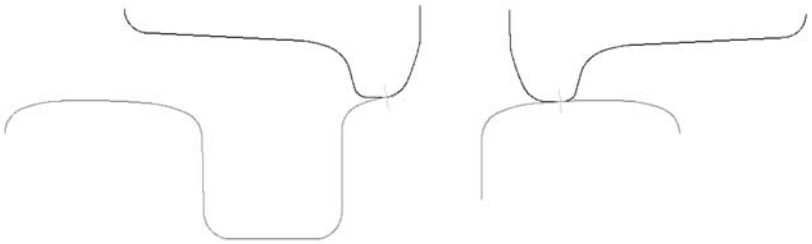

Figure 36 Flange climb derailment, wheel flange angle = 75 degrees, AOA = 20 mrad (no lubrication), W/R friction coefficient mu = 0.5, flangeway width = 1.89 in.

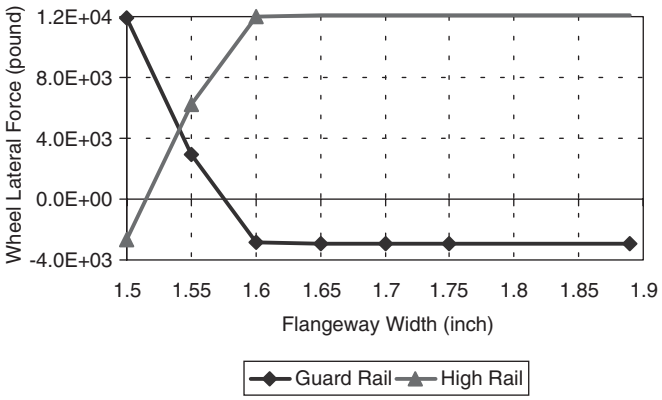

Figure 37 Guard rail W/R lateral forces, wheel flange angle = 75 degrees, AOA = 20 mrad, guard rail mu = 0.18, high-rail flange mu = 0.3.

- The three-dimensional W/R contact effect is significant at AOA higher than 58 mrad (corresponding to curves with about 100-ft radius).
- The flangeway width should increase by approximately the same amount as the gage is increased to keep the flange front clearance equal to the flange back clearance. Increasing only the gage leads to excessive wear on guard rails.
- Increasing gage or decreasing flangeway width leads to a tendency of increasing lateral W/R forces and wear on guard/girder/restraining rails because increasing gage increases the W/R flange front clearance and decreasing flangeway width decreases the flange back clearance. Both of these effects cause the guard/girder/restraining rail to contact the wheelset before the high rail contacts the flange face. Correspondingly, decreasing gage or increasing flangeway width leads to a tendency of increasing lateral W/R forces and wear on high rails.
- The flangeway width should increase with increasing guard rail height to keep the flange front clearance equal to the flange back clearance.
- The total rolling resistance increases with increasing guard rail height. However, the guard rail height effect on the maximum rolling resistance is relatively small.
- The guideline for guard rail lubrication is to keep low friction coefficients on the contact patches with high contact angles and high friction coefficients on the contact patches with low contact angles to ensure similar wear rates between the high rail and the guard rail.

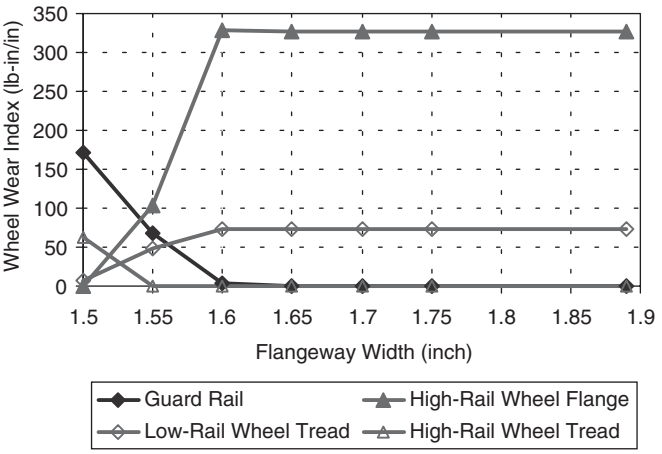

Figure 38 Guard rail W/R wear, wheel flange angle = 75 degrees, AOA = 20 mrad, guard rail mu = 0.18, high-rail flange mu = 0.3.

4.4 Girder Rail

Figure 39 shows a typical girder rail cross section used in transit systems, with the girder part 0.5 in. above the running rail top. The flangeway width is defined as in Figure 39. Table 5 shows the simulation parameters for girder rail.

4.4.1 Effect of Flangeway Width

Figure 40 shows the W/R forces and wear indices for a wheelset contacting on the girder rail with the parameters listed in Table 5. The optimal flangeway

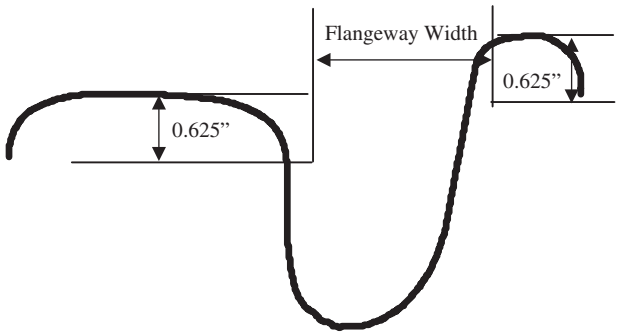

Figure 39 Girder rail cross section and flangeway width definition.

Table 5 W/R parameters for girder rail simulations

Parameters	Value
Wheel back-to-back distance	54.1875 in
Wheel maximum angle	75 deg
Wheel nominal radius	14 in
Running rail	AREMA 115-lb rail
Girder rail height	0.5 in above low-rail top
Gage	56.75 in
Wheelset AOA	20 mrad
W/R friction coefficients	Guard Rail 0.3, Running rail 0.5

width is 1.61 in., with a 63.9-degree contact angle on the high rail and a 77.2-degree contact angle on the girder, as Figure 41 (c) shows.

Instead of the whole cast structure of the girder rail, the two-piece strap guard rail (shown in Figure 5) could be convenient for optimal flangeway width adjustment through inserting shims between the web of the running rail and the strap guard.

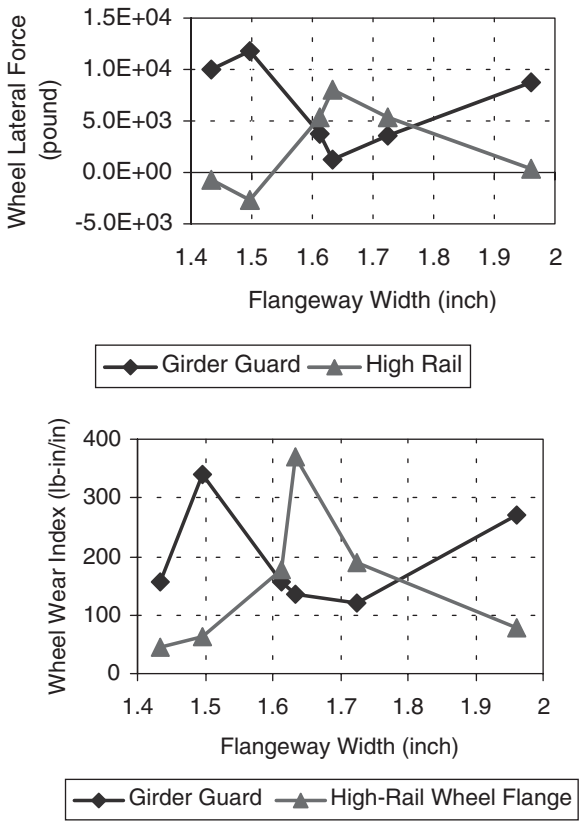

Figure 40 Girder rail W/R lateral forces and wear, wheel flange angle = 75 degrees, AOA = 20 mrad.

4.4.2 Effect of AOA/Track Curvature

Figure 42 shows the W/R forces and wear indices for a wheelset contacting the girder rail, with a 58-mrad AOA and the other parameters listed in Table 5. The optimal flangeway width for a 58-mrad AOA is about 1.68 in., 0.07 in. wider than the optimal flangeway width for a 20-mrad AOA; this is because of the three-dimensional wheel flange fattening effect at higher AOA (larger than 20 mrad).

4.4.3 Effect of Gage

Figure 43 shows the W/R forces and wear indices for a wheelset contacting a girder rail, with a 58-mrad AOA, a 0.25-in. gage increase (57-in. gage), and the parameters listed in Table 5. The compromise flangeway width for the 58-mrad AOA with a 0.25-in. gage increase is about 1.95 in., 0.27 in. wider than the flangeway width without a gage increase.

Because the girder portion of the rail is conformal to the wheel flange back, the W/R contact angle on the girder (77.1 degrees) is larger than the contact angle for the guard rail discussed in Section 4.3.5 (73.5 degrees). Other than that, the girder rail W/R contact geometry is similar to that of the guard rail. The conclusions from the girder rail simulations are therefore similar to those for guard rails.

4.5 Restraining Rail

Table 6 shows the simulation parameters for a 75-degree flange angle wheel negotiating a curve equipped with a restraining rail.

Figure 44 shows the W/R forces and wear indices for a wheelset contacting a restraining rail with the parameters listed in Table 6. There is no optimal flangeway width for these contact conditions because the contact angle of the wheel back on the restraining rail is 90 degrees, which is much larger than the contact angle on the flanging side of the wheel. Based on the methodology of "lubricating high flange angle with low friction coefficient" (as discussed in Section 4.3.5), the friction coefficient on the restraining rail is further decreased to 0.1; the optimal flangeway width is then obtained as 1.66 in., as Figure 45 shows. In order to allow for comparing the restraining rail simulations with the guard rail and girder rail simulations, a restraining rail friction coefficient of 0.3 was used for the restraining rail simulations unless otherwise specified.

(a) Flangeway width 1.433 in.

(b) Flangeway width 1.496 in.

(c) Flangeway width 1.613 in. (optimal).

(d) Flangeway width 1.634 in.

(e) Flangeway width = 1.725 in.

(f) Flangeway width 1.961 in.

Figure 41 Girder rail W/R contact animation, wheel flange angle = 75 degrees, AOA = 20 mrad.

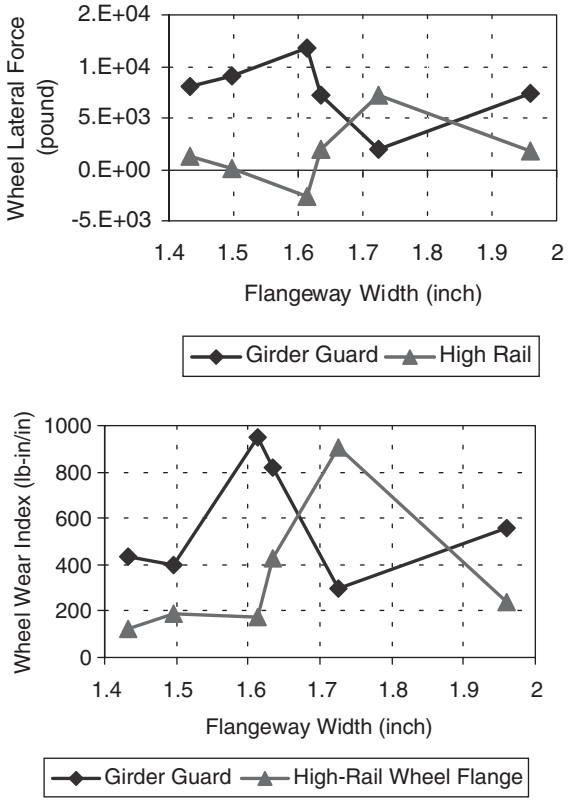

Figure 42 Girder rail W/R lateral forces and wear, three-dimensional wheel contour, AOA = 58 mrad.

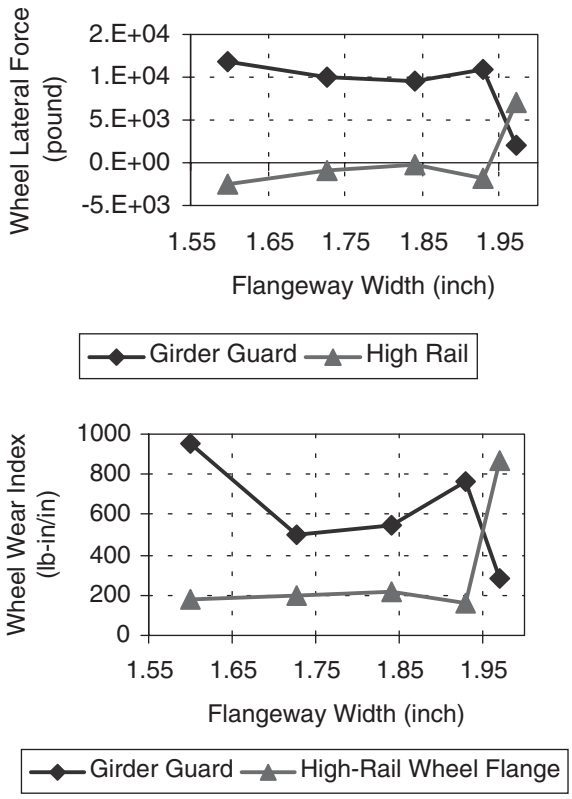

Figure 43 Girder rail W/R lateral forces and wear, three-dimensional wheel contour, AOA = 58 mrad, gage = 57 in.

4.5.1 Effect of Axle AOA/Track Curvature

Because the wear index can be adjusted through the friction coefficient, the optimal flangeway width for the restraining rail is mainly determined by the W/R lateral forces.

Figure 46 shows the W/R lateral forces for a wheelset with a 12-mrad AOA and the parameters listed in Table 6. The optimal flangeway width for wheelset with a 12-mrad AOA is 1.64 in., 0.02 in. smaller than the width for the 20-mrad AOA case.

For a wheelset with a 58-mrad AOA, the three-dimensional wheel contour had to be used in the simulation to take into account the three-dimensional contact effect. Figure 47 shows the W/R forces for a wheelset with a 58-mrad AOA, three-dimensional wheel contour, and the parameters listed in Table 6. The optimal flangeway width for the wheelset with a 58-mrad AOA is about 1.73 in., 0.07 in. wider than the wheelset with the 20-mrad AOA (because of the three-dimensional contact wheel flange fattening effect).

If the flange fattening effect is ignored and the two-dimensional wheel profile shape is used in the simulation, as Figure 48 shows, the optimal flangeway width is predicted to be about 1.77 in., 0.04 in. wider than the real optimal value.

The optimal flangeway width for restraining rails has to be increased with increasing axle AOA or track curvature because the three-dimensional con-

Table 6 W/R parameters for restraining rail simulations

Parameters	Value
Wheel back-to-back distance	54.1875 in
Wheel maximum angle	75 deg
Wheel nominal radius	14 in
Running rail	AREMA 115-lb rail
Restraining rail height	0.105 in above low-rail top
Gage	56.75 in
Wheelset AOA	20 mrad
W/R friction coefficients	Restraining rail 0.3, Running rail 0.5

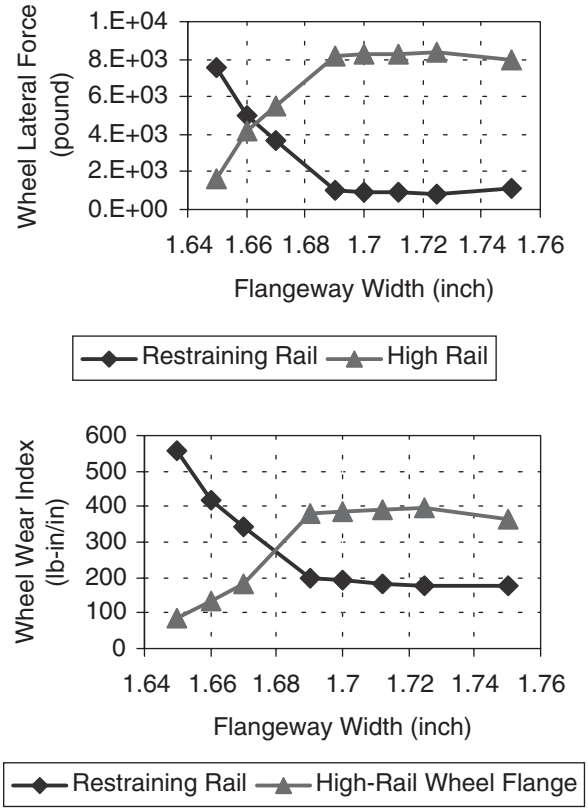

Figure 44 Restraining rail W/R lateral forces and wear, wheel flange angle = 75 degrees, AOA = 20 mrad.

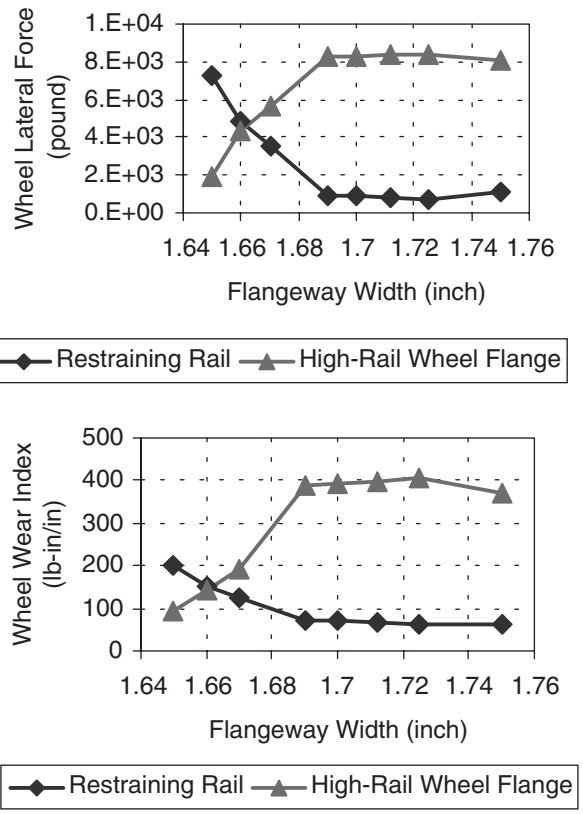

Figure 45 Restraining rail W/R lateral forces and wear, wheel flange angle = 75 degrees, AOA = 20 mrad, restraining rail mu = 0.1.

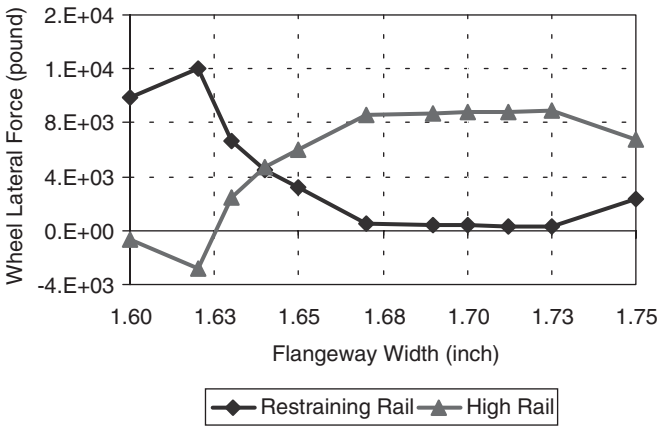

Figure 46 Restraining rail W/R lateral forces, wheel flange angle = 75 degrees, AOA = 12 mrad.

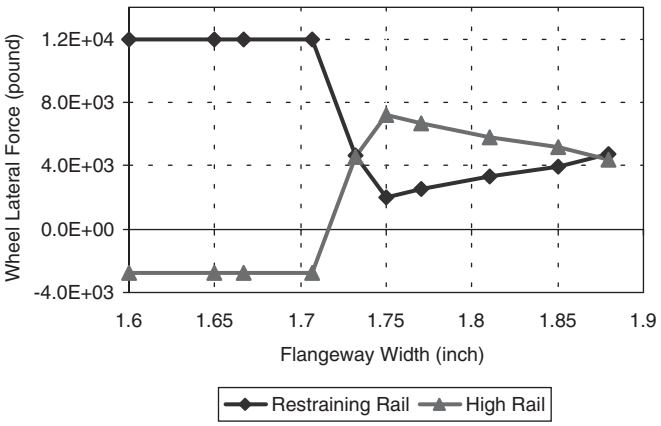

Figure 47 Restraining rail W/R lateral forces, three-dimensional wheel contour, AOA = 58 mrad.

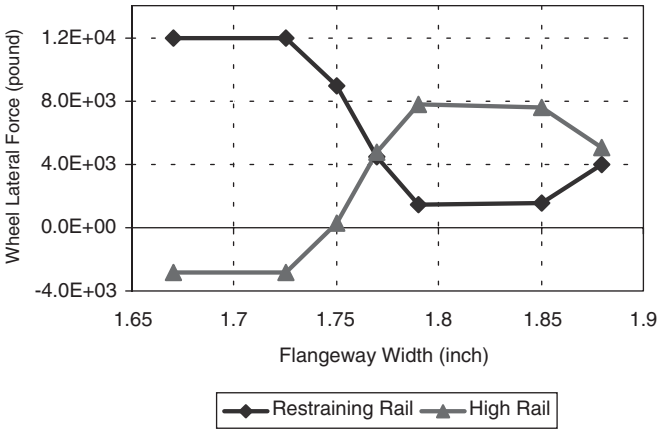

Figure 48 Restraining rail W/R lateral forces, wheel flange angle = 75 degrees, AOA = 58 mrad, two-dimensional wheel contour.

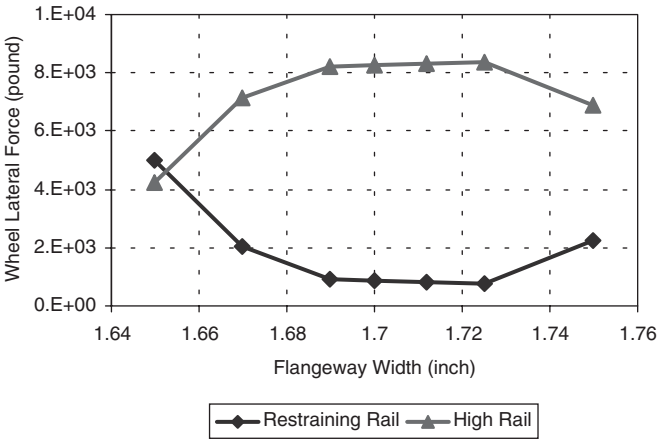

Figure 50 Restraining rail W/R lateral forces, wheel flange angle = 75 degrees, AOA = 20 mrad, restraining rail height = 0.02 in.

tact wheel back fattening effect is usually larger than that on the flange.

Because the restraining rail contacts on the wheel back, as described in Section 2.4, the three-dimensional contact effect increases significantly with increasing restraining rail height, but increases insignificantly for guard rails and girder rails. The restraining rail height effect is further discussed in Section 4.5.3.

4.5.2 Effect of Gage

Figure 49 shows the W/R forces for a wheelset with contact on the restraining rail, with 0.25-in. gage increase (57-in. gage) and the same parameters as the previous case (a wheelset with a 58-mrad AOA).

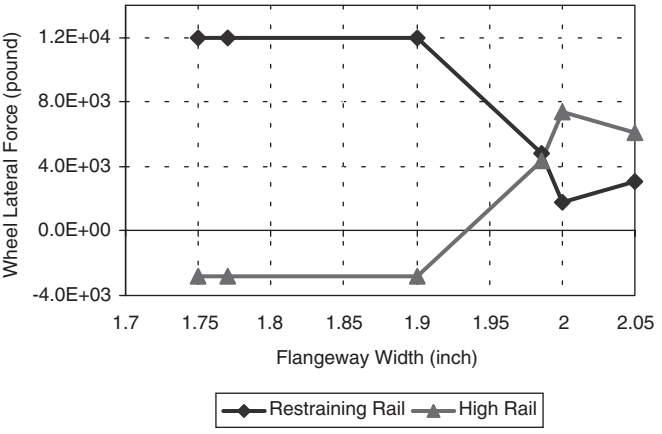

Figure 49 Restraining rail W/R lateral forces, three-dimensional wheel contour, AOA = 58 mrad, gage = 57 in.

The optimal flangeway width for 58-mrad AOA with 0.25-in. gage increase is about 1.99 in., 0.26 in. wider than the width without a gage increase.

The optimal flangeway width for restraining rails increases with increasing gage, with the increase in flangeway width approximately equal to the increase in gage.

4.5.3 Effect of Restraining Rail Height

Figures 50, 51, and 52 show the W/R forces for a wheelset contacting a restraining rail, with the restraining rail located 0.02, 0.315, and 0.515 in. above the low-rail top with the parameters listed in Table 6. The optimal flangeway widths are 1.65, 1.68, and 1.70 in., respectively, for a wheelset with 20-mrad AOA. The optimal flangeway width increases approx-

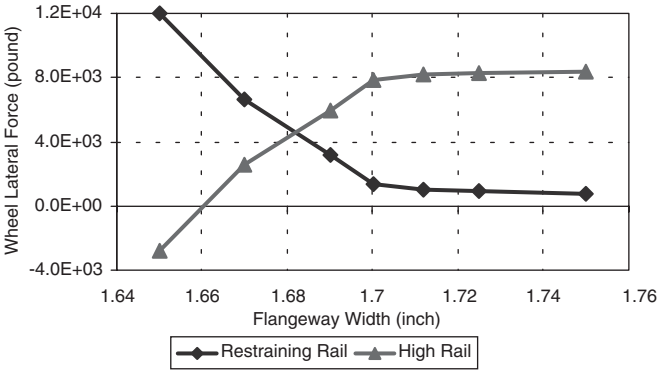

Figure 51 Restraining rail W/R lateral forces, wheel flange angle = 75 degrees, AOA = 20 mrad, restraining rail height = 0.315 in.

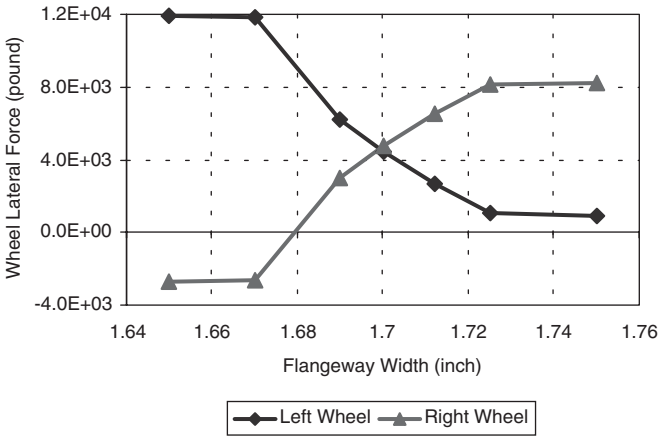

Figure 52 Restraining rail W/R lateral forces, wheel flange angle = 75 degrees, AOA = 20 mrad, restraining rail height = 0.515 in.

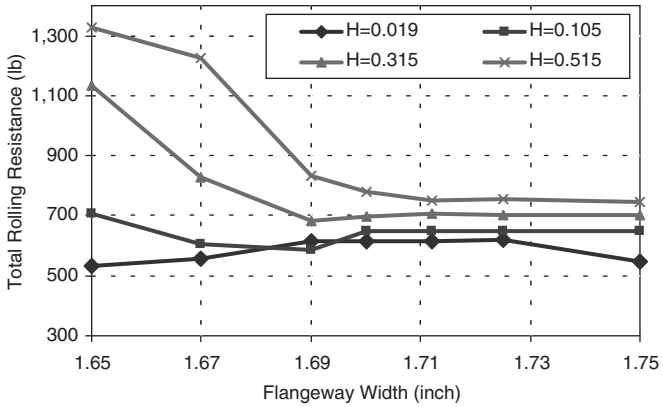

Figure 54 Effect of restraining rail height on rolling resistance, wheel flange angle = 75 degrees, AOA = 20 mrad.

imately linearly with increasing restraining rail height (see Figure 53).

Figure 54 shows the effect of different restraining rail heights on rolling resistance. Clearly, the higher the restraining rail, the greater the rolling resistance and W/R wear. The restraining rail should be installed low enough to mitigate excessive wear and decrease rolling resistances without compromising other safety concerns.

4.5.4 Effect of Lubrication

The contact angle between the wheel back and the restraining rail is 90 degrees, which is higher than that for guard rails and girder rails; therefore, according to the rule of "high contact angle with low friction coefficient," the restraining rail should be lubricated to obtain lower friction coefficients. On the basis of the limited number of simulations for a wheel with a 75-degree flange angle discussed in this digest, it appears that the guard rail and girder rail should be lubricated to obtain a friction coefficient that is 60 percent of the friction coefficient on the high-rail gage face flange. The restraining rail, however, should be lubricated to obtain a friction coefficient that is 20 percent of the friction coefficient on the high-rail gage face flange.

Figure 55 shows the effects of different restraining rail lubrication conditions on rolling resistance. Clearly, rolling resistance increases with the increase of the W/R friction coefficient. The rolling resistance decreases dramatically when the restraining rails are lubricated at the 0.15 friction coefficient level.

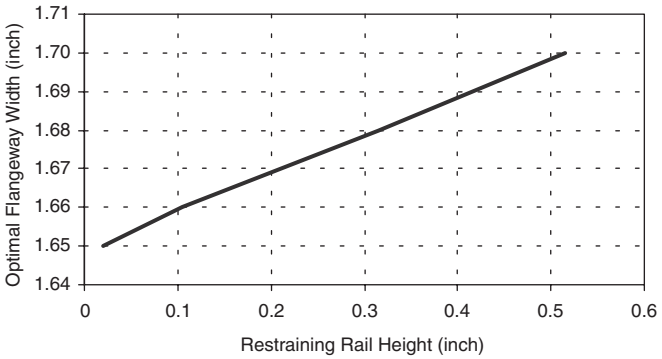

Figure 53 Effect of restraining rail height on flangeway width, wheel flange angle = 75 degrees, AOA = 20 mrad.

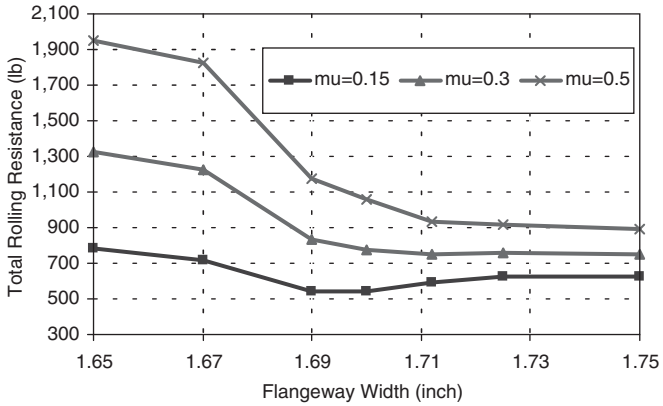

Figure 55 Effect of restraining rail lubrication on rolling resistance, wheel flange angle = 75 degrees, AOA = 20 mrad.

4.5.5 *Effect of Wheel Profile Shape*

To investigate the effect of different W/R profile combinations on W/R lateral forces and wear, simulations for a 63-degree flange angle wheel contacting a restraining rail were conducted using the parameters listed in Table 7.

The 63-degree flange angle wheel is used for a heavy rail transit system, whereas the 75-degree flange angle wheel is used for a light rail transit system. Thus, the wheel back-to-back distance and track gage parameters for these two wheelsets are different for meeting the requirements of different vehicles and track standards. However, to facilitate comparison of W/R force and wear, the same load and operating simulation conditions were used for the 63-degree flange angle wheel and the 75-degree flange angle wheel.

As Figure 56 shows, the flangeway width needed to balance lateral forces between the guard rail and the high rail is about 2.79 in.; however, the restraining rail wear index is always higher than the wear index of the high rail regardless of the flangeway width.

The high wear on the restraining rail is caused by the high contact points on the wheel back, as shown by the animation diagram in Figure 57. The radius on the wheel back (R_2) in Figure 6, where the flange shape ends and the wheel back plane starts, is 14.2374 in. for the 63-degree flange angle wheel, 0.2374 in. larger than the wheel back radius for the 75-degree flange angle wheel, which is 14 in. Even though the restraining rail height above the running rail top for the 63-degree flange angle wheel is almost equal to the restraining rail height of the 75-degree flange angle wheel, its contact points, longitudinal shift (L), and rolling radius increase with the wheel back radius (R_2) as Figure 6 shows. The larger rolling radius difference and longitudinal shift lead to the high creepages and wear.

Table 7 W/R parameters for simulations of the 63-degree flange angle wheel/ restraining rail

Parameters	Value
Wheel back-to-back distance	53.3125 in
Wheel maximum angle	63 deg
Wheel nominal radius	14 in
Running rail	AREMA 115-lb rail
Restraining rail height	0.103 in above low-rail top
Gage	57.25 in
Wheelset AOA	20 mrad
W/R friction coefficients	Restraining rail 0.3, Running rail 0.5

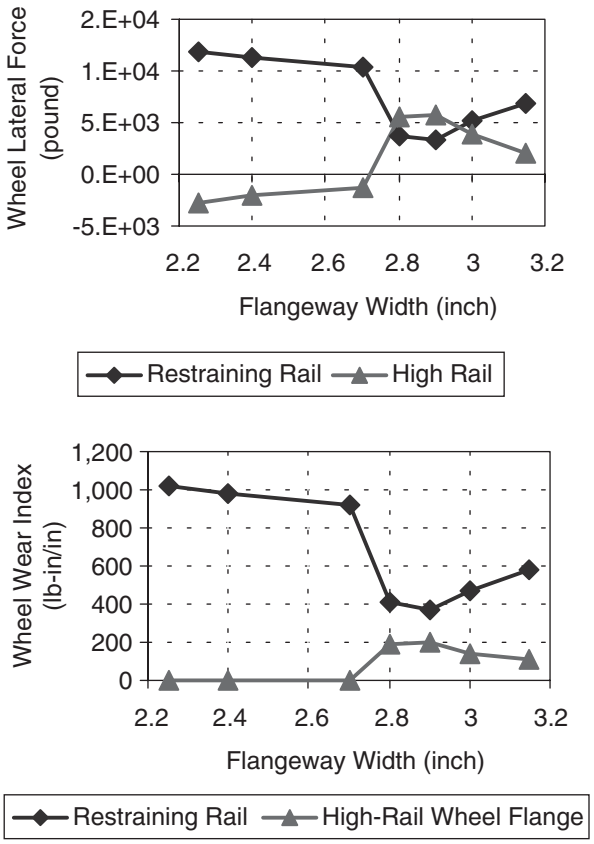

Figure 56 Restraining rail W/R lateral forces and wear, wheel flange angle = 63 degrees, AOA = 20 mrad.

If the restraining rail height is 0.23 in. below the running rail top, the optimal flangeway width is 2.73 in., with equal wear and lateral forces between the restraining rail and the high rail, as Figure 58 shows. The lower contact point shown in Figure 59, as compared with the contact point shown in Figure 57, leads to a lower longitudinal shift (L), as Figure 6 shows, and lower creepages and wear.

A comparison of Figure 44 and Figure 58 shows that under the same load and lubrication conditions the high-rail wear index for the 75-degree flange angle wheel is higher than the high-rail wear index for 63-degree flange angle wheel. These simulation results could explain wear observed when converting from a low flange angle wheel design to a high flange angle wheel design to avoid flange climb derailments. The use of the optimized guard/girder/restraining

Figure 57 Restraining rail W/R animation, wheel flange angle = 63 degrees, AOA = 20 mrad, flangeway width = 2.8 in.

rail designs described here could help mitigate this excessive W/R wear.

5 VALIDATION THROUGH TRANSIT VEHICLE SIMULATIONS

The above analyses assume that the wheelset AOA remains constant during the entire simulation, including flange climb and flange back climb. The wheelset AOAs in vehicles vary during curve negotiation depending on the truck design and steering capability. To validate the optimal flangeway width predictions described in Section 4, results from vehicle simulations with a 75-degree flange angle wheel contacting guard/girder/restraining rails are presented in this section.

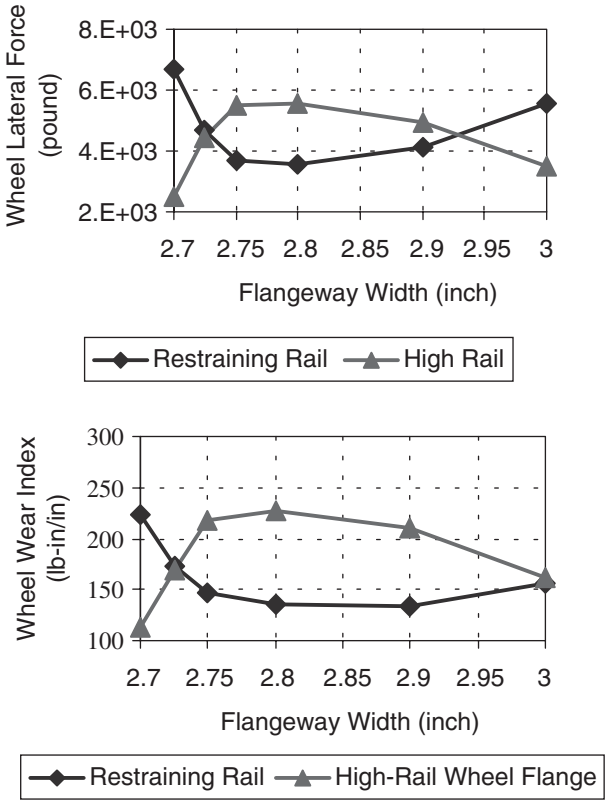

Figure 58 Restraining rail W/R lateral forces and wear, wheel flange angle = 63 degrees, AOA = 20 mrad, restraining rail height = –0.23 in.

The vehicle modeled is a typical articulated low-floor light rail transit vehicle. It is composed of three car bodies and three trucks. The end car bodies are each mounted on a single truck at one end and connected to an articulation unit at the other end. The center car body is the articulation unit riding on a single truck equipped with independent rotating wheels. The principal dimensions of the vehicle are the following:

- rigid wheel base of 74.8 in.;
- solid wheel diameter of 28 in., independent rotating wheel diameter of 26 in.; and
- truck centers of 289.4 in.

Overall, a total of 26 bodies and 138 connections were used in the NUCARS® model. Tables 4, 5, and 6 show the W/R parameters used for the guard/girder/restraining rails, respectively. The same model was used in a previous TCRP project to analyze flange climb derailments (*1*).

The track inputs include a right hand smooth curve with a 290-ft radius, 3.25-in. superelevation, and 3-in. cant deficiency (21.27 mph). The spiral and curve are long enough to ensure that the vehicle achieves an equilibrium position while negotiating the curve.

The optimal flangeway width, based on the leading axle W/R forces and wear, is examined as compared with the single wheelset simulation results.

5.1 Vehicle Negotiating a Curve with a Guard Rail

As Figure 60 shows, the vehicle simulation predicts that the optimal flangeway width for the guard rail with 0.2-in. height is about 1.57 in., which is consistent with the optimized value predicted by the single wheelset simulation in Figure 25. The wheelset AOA in the equilibrium position is about 20.1 mrad.

Figure 59 Restraining rail W/R animation, wheel flange angle = 63 degrees, AOA = 20 mrad, restraining rail height = –0.23 in., flangeway width = 2.73 in.

5.2 Vehicle Negotiating a Curve with a Girder Rail

As Figure 61 shows, the vehicle simulation predicts the optimal flangeway width for the girder rail is about 1.61 in., which is consistent with the optimized value predicted by the single wheelset simulation in Figure 40. The wheelset AOA in the equilibrium position is about 20.3 mrad.

5.3 Vehicle Negotiating a Curve with a Restraining Rail

As Figure 62 shows, the vehicle simulation predicts (for a restraining rail with a 0.02-in. height) that the optimal flangeway width is about 1.655 in., which is consistent with the optimized value predicted by the single wheelset simulation in Figure 50. The wheelset AOA in the equilibrium position is about 20.2 mrad.

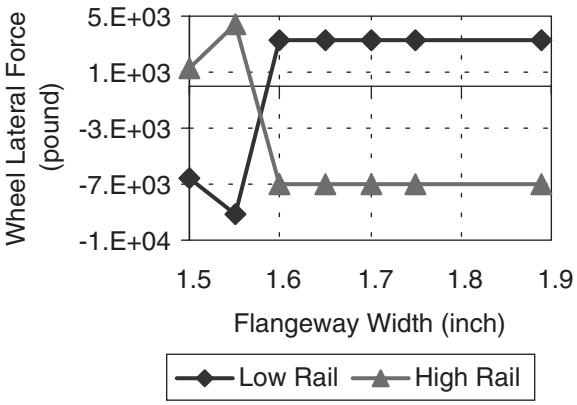

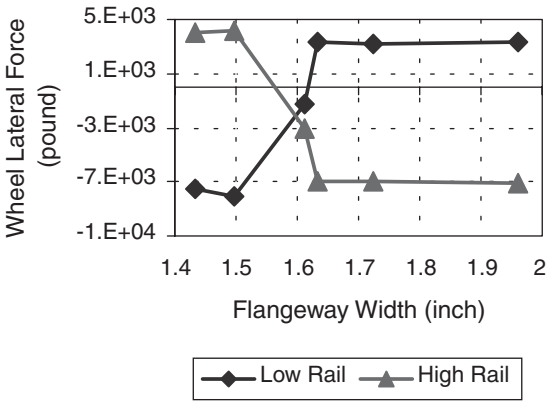

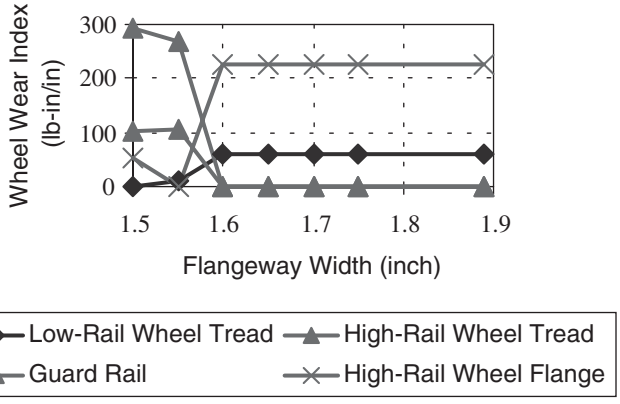

Figure 60 Guard rail W/R lateral forces and wear, wheel flange angle = 75 degrees, 290-ft radius curve, guard rail height = 0.2 in. above running rail.

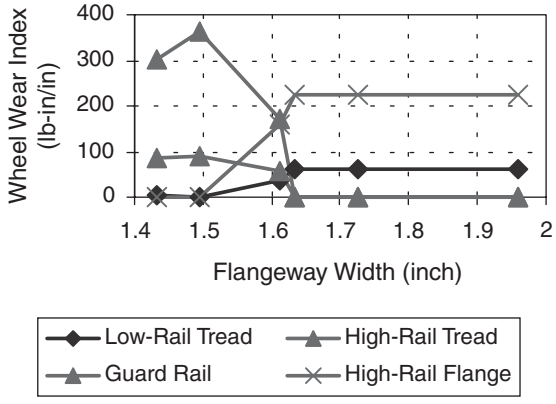

Figure 61 Girder rail W/R lateral forces and wear, wheel flange angle = 75 degrees, 290-ft radius curve, girder rail height = 0.5 in.

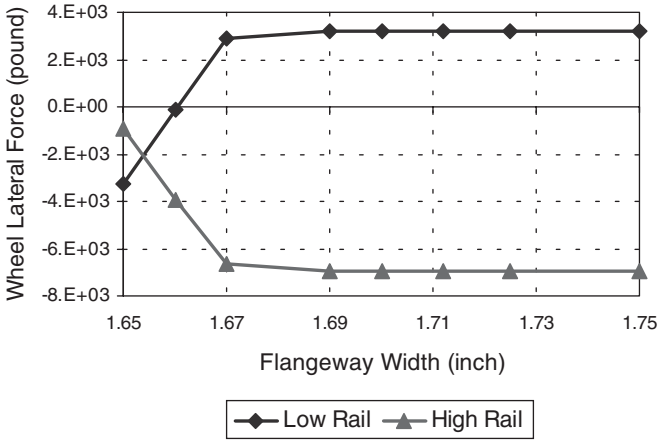

Figure 62 Restraining rail W/R lateral forces, wheel flange angle = 75 degrees, restraining rail height = 0.02 in., 290-ft radius curve.

The vehicle simulation results show that the wheelset AOA is mainly determined by the truck and curve geometry. For most transit vehicle trucks without severe wear on the components, the wheelset steering effect on AOA is relatively small, unless a very soft primary suspension or a forced steering suspension is used. The single wheelset model with constant AOA and optimization methodologies developed in this report is therefore valid for most guard/girder/restraining rail design and optimization applications.

6 VEHICLE SAFETY AND WEAR ANALYSIS FOR GUARD/GIRDER/RESTRAINING RAIL INSTALLATION

Transit systems use guard/girder/restraining rails to mitigate safety and component wear issues. Cost is also a factor in the process of deciding where to apply guard/girder/restraining rails and selecting the appropriate technology.

A cost-benefit analysis is not included in the scope of this study; therefore, this section of the report focuses on vehicle dynamics, safety, and wear analysis for various vehicle types to provide guidelines to aid in the implementation of guard/girder/restraining rails.

6.1 Safety Analysis

A common safety risk during curve negotiation for transit vehicles is flange climb derailment. The vehicle suspension arrangement and wheel flange angle have the most important effect on this derailment mechanism, as shown by the results obtained from the simulations described here.

Two types of light rail transit vehicles were used in the simulations. The first light rail vehicle model (LRV1) is a low-floor articulated vehicle (described in Section 5). The second model (LRV2) represents a typical high-floor articulated vehicle composed of two car bodies and three trucks. The two car bodies articulate on the middle truck, with all three trucks having solid wheelsets.

The track geometry used in the simulations consisted of a downward vertical cusp of 1.25-in. amplitude on the high rail combined with 0.875-in. outward lateral alignment cusp on the high rail and an inward cusp of 0.25-in. amplitude on the low rail. These irregularities of the track geometry were composed of 31-ft wavelengths with a 1-cosine shape on a curve with a 1,000-ft radius.

The W/R profile combinations used in the simulation were the 63- or 75-degree flange angle wheel on standard AREMA 115-lb/yd rail. The W/R friction coefficient used in the simulation was 0.5.

The two vehicle models and the track perturbation shape are the same as those used in a previous TCRP study on flange climb derailment (*1*).

Figure 63 shows the L/V ratios on the outside wheel on the third axle of both vehicles. The independent rotating wheels of the LRV1 vehicle with a 63-degree flange angle wheel profile derailed at 25 mph. To improve flange climb safety at speeds of 25 mph and above, a guard rail should be installed on curves with a radius of 1,000 ft and smaller for this vehicle and wheel profile combination. An alternative method is to change the wheel flange angle from 63 degrees to 75 degrees to increase the wheel flange climb resistance ability, as shown in the graph labeled LRV1/75Deg. The LRV1 vehicle with a 75-degree flange angle wheel profile doesn't derail until its L/V ratio exceeds the Nadal value. However, the LRV2 vehicle with both wheel profiles doesn't derail up to 55 mph, which means guard rail installation can be relaxed for curves of less than 1,000 ft in radius for this vehicle's suspension arrangement.

Because each transit system has a different fleet and different wheel and rail profile standards, guard rail utilization has to be optimized on a case-by-case basis to take into account the different vehicle performance characteristics.

To ensure safety, the guideline for guard rail utilization on curves is to install guard rails wherever the L/V ratio and flange climb distance exceed the L/V

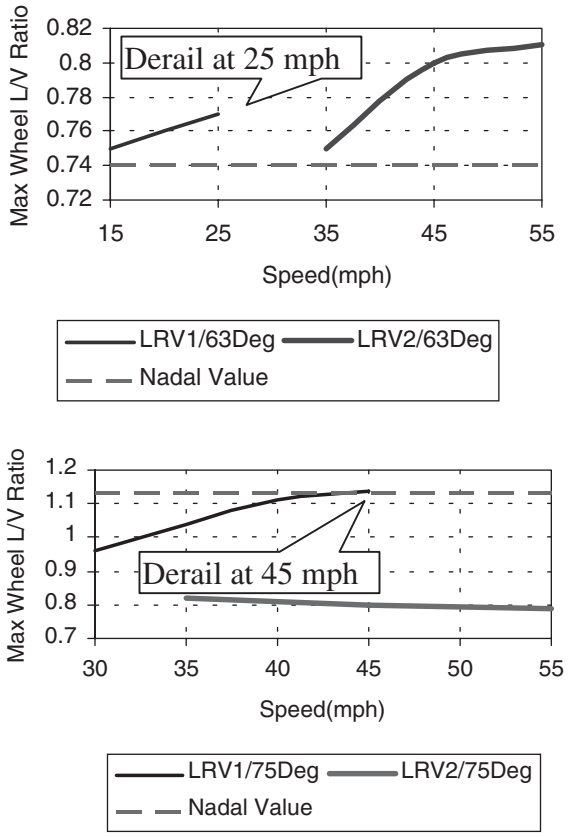

Figure 63 Effect of vehicle suspension arrangement and W/R contact angle on derailment.

ratio and climb distance safety criteria as proposed in *TCRP Report 71: Track-Related Research—Volume 5: Flange Climb Derailment Criteria and Wheel/Rail Profile Management and Maintenance Guidelines for Transit Operations* (*1*).

6.2 Wear Analysis

6.2.1 Damage Functions

Tests and simulations have shown that the NUCARS® W/R wear index is a good indicator of a vehicle's propensity to cause rolling contact fatigue (RCF) and wear. Figure 64 shows two W/R damage functions—crack RCF and wear components—developed by the Transportation Technology Center, Inc. (TTCI), based on laboratory experimental results (*9*).

To convert the damage functions shown in Figure 64 into a cost function, four regions need to be considered:

1. For a wear index greater than 0 lb-in./in., but less than or equal to 3.4 lb-in./in., RCF damage is zero because insufficient energy is being transmitted to the rail to exceed the shakedown limit. There are no maintenance or renewal costs associated with RCF or wear.
2. For a wear index greater than 3.4 lb-in./in. but less than or equal to 14.6 lb-in./in., RCF is removed by grinding. The amount of grinding is proportional to the amount of RCF damage. Eventually, enough material is ground from the head of the rail to require the rail to be renewed.
3. For a wear index greater than 14.6 lb-in./in. but less than or equal to 39.4 lb-in./in., less grinding is required to remove RCF because some is removed by wear. Grinding and wear combine to remove material from the head of the rail, and the rail eventually requires renewal.
4. For a wear index greater than 39.4 lb-in./in., grinding is no longer required because RCF is being removed by wear. Eventually the wear reaches the point where the rail requires renewal.

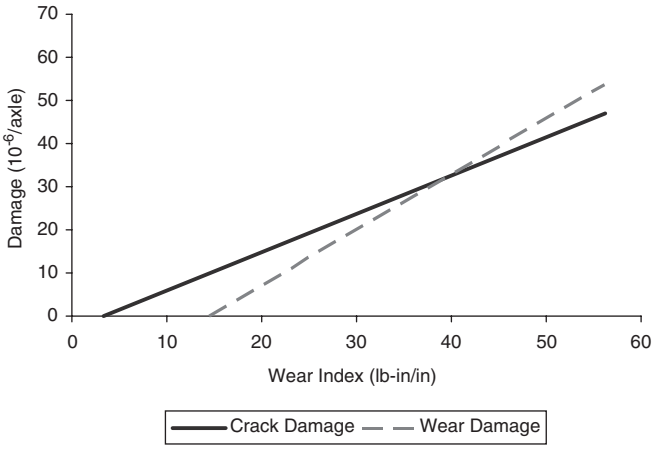

Figure 64 Rail damage functions.

The W/R wear is significant when the wear index exceeds 39.4 lb-in./in. Assuming that rail renewal cost is higher than the cost of grinding, keeping the wear index lower than 39.4 lb-in./in. could save cost based on these damage functions. For example, the cost for a high rail with a wear index of 70 lb-in./in. without guard rails could be higher than the cost of a high rail with a wear index of 38 lb-in./in. and guard rail with wear index of 38 lb-in./in., assuming the guard rail materials and installation costs are lower than the costs associated with high-rail maintenance and replacement.

These rail damage functions also provide evidence for the concept of guard rail parameter optimization, which uses the strategy of mitigating the excessive wear on high rails and sharing the wear between high rails and guard rails.

6.2.2 Run Matrix and Results

Four types of hypothetical transit cars representing two types of heavy rail and two types of light rail transit vehicles with the 63- and 75-degree flange angle wheel profiles have been modeled using NUCARS®. The two light rail vehicle models, LRV1 and LRV2, are described in Section 6.1. The two heavy rail vehicle models (HRV1 and HRV2) are composed of one car body and two trucks with secondary airbag suspensions. The differences between the HRV1 and HRV2 models are (1) that the HRV2 vehicle uses a rigid H-frame truck, whereas the HRV1 vehicle uses an articulated truck frame, and (2) that the HRV1 vehicle has cylindrical bushing, whereas the HRV2 vehicle has a chevron primary suspension.

The LRV1 and LRV2 vehicle models and the HRV2 vehicle model are the same models used in a previous TCRP study on flange climb derailment (*1*).

The curvature, superelevation, and running speed used in the wear analysis simulations are listed in Table 8. The track gage was varied from 56.25 to 57 in. depending on vehicle type and W/R profiles. The speeds used in the simulation produced a 1-in. cant deficiency for the curve of interest.

The W/R profile combinations used in the simulation were the 63- or 75-degree flange angle wheel on standard AREMA 115-lb/yd rail. The W/R friction coefficient used in the simulation was 0.5.

Figure 65 shows the wear indices on the leading axle wheels of different types of vehicles and wheel profile combinations without the use of guard rails. Clearly, the wear index difference between the high rail and the low rail for 75-degree flange angle wheels is larger than that for the 63-degree flange angle wheels. Therefore, there is a greater need for guard/girder/restraining rails or high-rail lubrication on sharp curves for transit systems using 75-degree flange angle wheels because higher flange angle wheels wear the high rail faster than lower flange angle wheels.

Table 8 Wear simulation parameters

Curve Radius (ft)	Curvature (deg)	Superelevation (in)	Speed (mph)
250	22.92	0	7.87
500	11.46	0	11.12
750	7.64	4	30.66
817	7.01	4	32.00
955	6.00	4	34.60
1,145	5.00	4	37.88
1,430	4.01	4	42.34
1,910	3.00	4	48.93

Table 9 shows the wheel wear indices predicted for the high rail, corresponding to the minimum radius curve requiring guard rail installation on different transit systems. Wheel wear indices increase with wheel flange angles and axle loads.

All of these wear indices are close to or greater than the 39.4 lb-in./in. limit of the rail damage functions shown in Figure 64, which indicates that the rail starts to wear significantly. The wear index limit may not be necessarily the same as in Figure 64 because the damage function is material related.

The consistency between the damage functions and simulation results for vehicles in different transit systems shows that the rail damage functions and simulation results can be used for the wear and economic analyses.

The wear index is an important index for the evaluation of rail wear on curves; however, the minimum curvature requiring guard rail installation needs to be determined through safety and economic analyses. The wear indices for different vehicles provide input data for an economic analysis. The wear index is the wear of one wheel or one vehicle passing the rail; the real W/R wear is the total wear accumulation of all trains over time. The economic analysis depends not only on wear indices but also on many other factors, such as traffic volume, material and labor cost, and inflation. Consideration of these other factors is outside of the scope of this study.

7 CONCLUSIONS

The effects of three-dimensional wheel/guard/girder/restraining rail contact geometry and guard/girder/restraining rail installation parameters—including flangeway width and height, lubrication, track curvatures, track gage, and vehicle types on W/R forces and wear—have been investigated through NUCARS® simulations. A number of important conclusions including guidelines for

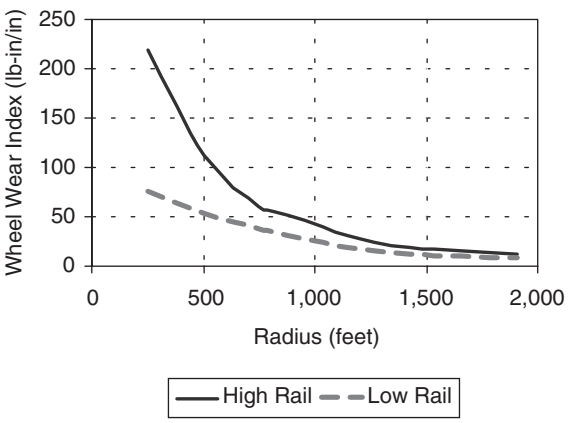

(a) LRV1: 63-degree flange angle wheel.

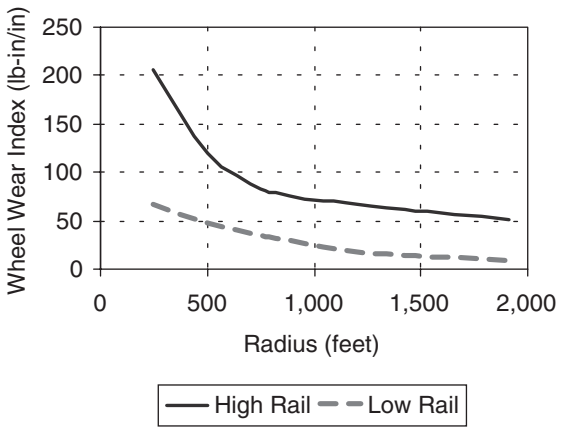

(b) LRV1: 75-degree flange angle wheel.

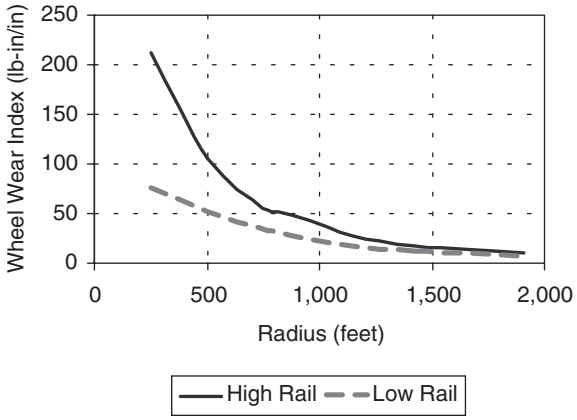

(c) LRV2: 63-degree flange angle wheel.

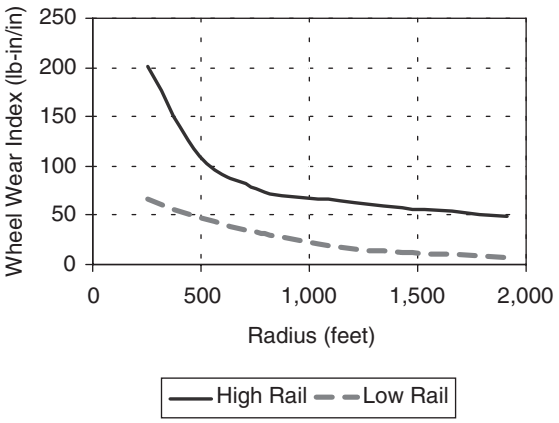

(d) LRV2: 75-degree flange angle wheel.

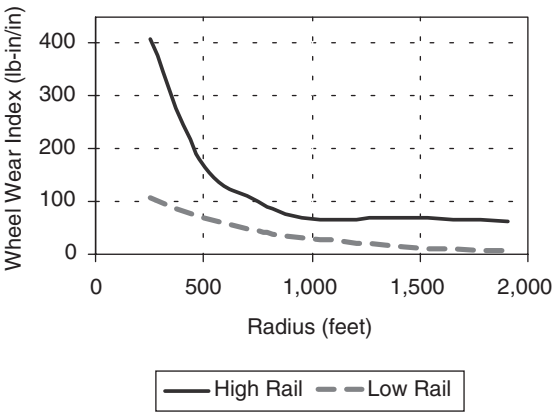

(e) HRV1: 63-degree flange angle wheel.

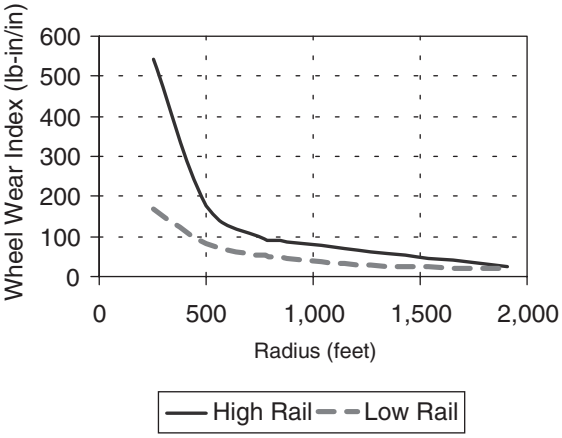

(f) HRV2: 63-degree flange angle wheel.

Figure 65 Wear indices for different types of vehicles and wheel profiles.

Table 9 Wheel wear index corresponding to curves without guard rails in six transit systems

Case	A	B	C	D	E	F
Car Type	**LRV 1**	**LRV 1**	**LRV 2**	**LRV 2**	**HRV 1**	**HRV 2**
Wheel maximum flange angle (deg)	63	75	63	75	63	63
Min. curve radius for installation of guard rail (ft)	1,000	1,000	1,000	1,000	800	750
Axle load (lb)	16,940	16,940	16,439	16,439	27,700	27,911
Leading axle wheel wear index (lb-in/in)	46	72	43	68	97	99

optimized guard/girder/restraining rail installation and design can be drawn from this work:

- The optimal guard/girder/restraining rail installation, leading to a balance of lateral W/R forces as well as a balance of wear between the high rail and the guard/girder/restraining rail, can be achieved through the control of flangeway width and W/R friction coefficients.
- The optimal flangeway width depends on the wheel profile shape including flange back profile, wheel back-to-back distance, track gage, guard/girder/restraining rail profile shapes, installation height, and wheelset AOA or the track curvature.
- The optimal flangeway width makes the flange front W/R clearance between the wheel flange face and the high rail equal to the flange back clearance between the wheel flange back and the guard rail. (See Figure 1.)
- A wide flangeway width leads to high lateral forces and wear on the high rail and increases high-rail flange climb derailment risk.
- A narrow flangeway width leads to high lateral forces and wear on the guard/girder/restraining rail and increases low-rail flange back climb derailment risk.
- The flangeway width should increase with the wheelset AOA and track curvature for AOA larger than 20 mrad (corresponding to curves with about 290-ft radius) if the three-dimensional flange back fattening effect is larger than the fattening effect on the maximum flange angle face (this situation applies to most W/R contact cases).
- The three-dimensional W/R contact effect is significant at AOA higher than 58 mrad (corresponding to curves with about 100-ft radius).
- The flangeway width should increase by approximately the same amount as the track gage increases to keep the flange front clearance equal to the flange back clearance. Increasing only the gage leads to excessive wear on the guard/girder/restraining rails.
- Increasing gage or decreasing flangeway width leads to a tendency of increasing lateral W/R forces and wear on guard/girder/restraining rails because increasing gage increases the W/R flange front clearance, and decreasing flangeway width decreases the flange back clearance, causing the guard/girder/restraining rail to contact the wheelset before the high rail contacts the flange face. Correspondingly, decreasing gage or increasing flangeway width leads to a tendency of increasing lateral W/R forces and wear on high rails.
- The flangeway width should increase with the increase of the guard/girder/restraining rail height to keep the flange front clearance equal to the flange back clearance.
- The total rolling resistance increases with the increase of the guard/girder/restraining rail height. However, the height effect for guard and girder rails on W/R wear and rolling resistance is relatively small compared with that of the restraining rail.
- The restraining rail height has a significant effect on rolling resistance and W/R wear. The restraining rail should be installed low enough to mitigate excessive wear and decrease rolling resistances without compromising other safety concerns.
- Lubrication on the high-rail gage face and guard/girder/restraining rail significantly reduces the W/R wear and rolling resistances. To achieve similar wear rates between the high rail and the guard rail, the guideline for rail lubrication with guard rail is to produce low friction coefficients on the contact patches in the presence of high contact angles and relatively

high friction coefficients on the contact patches in the presence of low contact angles.
- The wear for wheels with higher flange angles is more severe than those with lower flange angles under the same running and load conditions. The optimized guard/girder/restraining rail designs could provide solutions to excessive W/R wear.
- To ensure safety, the guideline for guard rail installations on curves is to install guard/girder/restraining rails wherever the wheel L/V ratio and flange climb distance exceed the wheel L/V ratio and climb distance criteria as proposed in *TCRP Report 71:Track-Related Research—Volume 5:Flange Climb Derailment Criteria and Wheel/Rail Profile Management and Maintenance Guidelines for Transit Operations* (*1*). Either tests or simulations can provide the L/V ratio and climb distance.
- The consistency between the damage functions (*9*) and simulation results for vehicles in different transit systems shows that the rail damage functions and simulations can be used for W/R wear and economics analysis.

It is suggested that these guidelines and the optimization designs and methodologies for guard/girder/restraining rails be validated through field tests.

8 DISCUSSION AND FUTURE WORK

8.1 Discussion

The study presented in this digest provides concepts, techniques, and procedures to determine the optimal flangeway width for guard/girder/restraining rails. Although new wheel and new rail profiles were used in the study, the same approach can be used to determine the optimal flangeway widths for any combination of new or worn W/R profiles. For an existing transit system, the distribution of new and worn wheel shapes in the system needs to be considered in determining the optimal flangeway width.

The optimal flangeway width is determined for the guard/girder/restraining rail installation. With the optimal flangeway width, the high-rail flange and the guard/girder/restraining rail will wear at the same rate in the initial stage. As wear increases, the W/R profiles change.

It has been stated that increasing gage and reducing flange thickness have the same effect on W/R forces and wear as decreasing flangeway width. Therefore, thinner wheel flanges caused by flange face wear and wider gage caused by high-rail gage face wear have the equivalent effect of decreasing flangeway width, while wheel flange back and guard rail wear have the equivalent effect of increasing flangeway width. Under ideal wear conditions, as the flangeway width increases with wear, the optimal force and wear condition is maintained with alternating wear of the guard/girder/restraining rail and the high-rail gage face, as Figure 66 illustrates.

If a guard/girder/restraining rail is not installed with the optimal flangeway width, the guard/girder/restraining rail or the high rail may eventually wear into the dimensions that produce balanced forces and wear. However, during the initial wear period, the forces and wear will be concentrated at either the high rail or the guard/girder/restraining rail. This initial wear can significantly reduce the effective life of rails if the initial flangeway width selected is too far from the optimal value.

Wear limits for flangeway width should also be determined for track maintenance purposes. Except for the considerations of rail head loss limits, wheel flange thickness limits, and guard/girder/restraining rail wear limits related to the strength of these elements, the effectiveness of the flangeway width in reducing the risk of flange climb derailment and reducing the severity of high-rail wear should be the major concerns. Investigation of flangeway wear limits is proposed for the next stage of study (discussed in the following section).

It is expected that for the optimized guard/girder/restraining rail structures, the maintenance tolerances

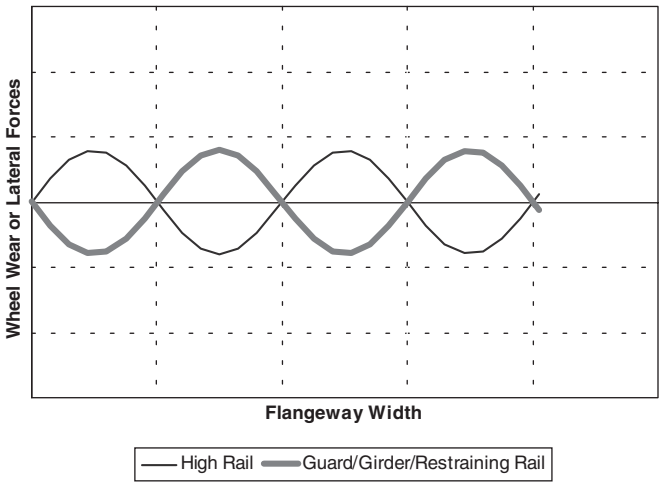

Figure 66 Dynamic balance of W/R forces and wear with guard/girder/restraining rails.

for the flangeway widths could be relaxed because of the dynamic balance characteristics (see Figure 66).

8.2 Future Work

The wear limit of the flangeway should be further studied to consider the effects of worn wheel and rail including the effect of guard/girder/restraining rail geometries.

The dynamic balance postulate and the guidelines predicted in Section 7 need to be further validated through the measurements of W/R forces and profile shapes.

The following approaches for future work are proposed:

- Conduct simulations to determine the wear limits of the flangeway and the effects of wear limits on flange climb derailment and high-rail wear.
- In conjunction with a transit system, install guard/girder/restraining rails on two similar segments of a single curve with one segment based on the guidelines and the other segment based on the current practice.
- Compare W/R lateral forces through strain gage measurement on the rails.
- Compare wear on high and low rails and the guard/girder/restraining rails every 3 months through accurate measurement of rail profiles.

This work would be greatly facilitated by the development of a wear model in a simulation program that automatically adjusts the W/R profile shapes as wear occurs.

REFERENCES

1. Wu, H., X. Shu, and N. Wilson. *TCRP Report 71: Track-Related Research—Volume 5: Flange Climb Derailment Criteria and Wheel/Rail Profile Management and Maintenance Guidelines for Transit Operations.* Transportation Research Board of the National Academies, Washington, D.C., 2005.
2. Cunney, E. G., and T.-L. Yang. *U.S. Transit Track Restraining Rail—Volume I: Study of Requirements and Practices.* UMTA-MA-06-0100-81-6. UMTA, Washington, D.C., December 1981.
3. Cunney, E. G., and T.-L. Yang. *U.S. Transit Track Restraining Rail—Volume II: Guidelines.* UMTA-MA-06-0100-81-7. UMTA, Washington, D.C., December 1981.
4. Parsons Brinckerhoff Quade & Douglas, Inc. *TCRP Report 57: Track Design Handbook for Light Rail Transit.* Transportation Research Board, National Research Council, National Academy Press, Washington, D.C., 2000.
5. Elkins, J. A., J. Peters, G. E. Arnold, and B. R. Rajkumar. *Steady State Curving and Wheel/Rail Wear Properties of a Transit Vehicle on the Tight Turn Loop.* UMTA-CO-06-0009-83-1. UMTA, Washington, D.C., December 1982.
6. Elkins, J. A., G. E. Arnold, B. R. Rajkumar, and A. J. Peters. "The Effect of a Restraining Rail on the Curving Behavior of Transit Vehicles." *Proc., 8th IAVSD Symposium on the Dynamics of Vehicles on Roads and Track.* Cambridge, MA, October 1983.
7. *NUCARS® Users Manual.* Transportation Technology Center, Inc. (a subsidiary of the Association of American Railroads). Pueblo, CO, 2006.
8. Reiff, R. P., N. Ruud, and S. F. Kalay. *TCRP Report 71: Track-Related Research—Volume 4: Friction Control Methods Used by the Transit Industry.* Transportation Research Board of the National Academies, Washington, D.C., 2005.
9. Tunna, John M. "Rail Surface Damage Usage Charging Model," TTCI Draft Report, Transportation Technology Center, Inc. (a subsidiary of the Association of American Railroads). Pueblo, CO, 2005.

AUTHOR ACKNOWLEDGMENTS

Useful data in this report have resulted from the generous efforts of many transit engineers and others. Valuable help and suggestions were provided by Anthony Bohara at SEPTA, Nabil Ghaly and Antonio Cabrera at MTA-NYCT, Earle Hughes at Ganett Fleming Transit & Rail System, Jim Dwyer and Jim LaBella at Port Authority of Allegheny County, Gavin Fraser at Booz-Allen Hamilton, and Tony Oriollo at MBTA. The authors also thank our colleagues Huimin Wu, John Tunna, and Stan T. Gurulé for proving valuable references and comments, as well as Program Manger Dingqing Li for project management and advice.

These digests are issued in order to increase awareness of research results emanating from projects in the Cooperative Research Programs (CRP). Persons wanting to pursue the project subject matter in greater depth should contact the CRP Staff, Transportation Research Board of the National Academies, 500 Fifth Street, NW, Washington, DC 20001.

THE NATIONAL ACADEMIES™
Advisers to the Nation on Science, Engineering, and Medicine

The nation turns to the National Academies—National Academy of Sciences, National Academy of Engineering, Institute of Medicine, and National Research Council—for independent, objective advice on issues that affect people's lives worldwide.
www.national-academies.org

TRB
Transportation Research Board
500 Fifth Street, NW
Washington, DC 20001